Inflationary attractors predictions for static neutron stars in the mass-gap region

S. D. Odintsov[1,2,*] and V. K. Oikonomou[3,†]

[1]*ICREA, Passeig Luis Companys, 23, 08010 Barcelona, Spain*
[2]*Institute of Space Sciences (ICE, CSIC), C. Can Magrans s/n, 08193 Barcelona, Spain*
[3]*Department of Physics, Aristotle University of Thessaloniki, Thessaloniki 54124, Greece*

(Received 4 February 2023; accepted 8 May 2023; published 17 May 2023)

In this work we study static neutron stars in the context of several inflationary models which are popular in cosmology. These inflationary models are nonminimally coupled scalar theories which yield a viable inflationary phenomenology in both Jordan and Einstein frames. By considering the constraints from inflationary theories, which basically determine the values of the potential strength, usually considered as a free parameter in astrophysical neutron star works, we construct and solve the Tolman-Oppenheimer-Volkoff equations using a solid Python-3 LSODA integrator. For our study we consider several popular inflationary models, such as the universal attractors, the R^p attractors (three distinct model values), the induced inflation, the quadratic inflation, the Higgs inflation and the a-attractors (two distinct model values) and for the following popular equations of state the WFF1, the SLy, the APR, the MS1, the AP3, the AP4, the ENG, the MPA1 and the MS1b. We construct the $M-R$ diagram and we confront the resulting theory with theoretical and observational constraints. As we demonstrate, remarkably, all the neutron stars produced by all the inflationary models we considered are compatible with all the constraints for the MPA1 equation of state. It is notable that for this particular equation of state, the maximum masses of the neutron stars are in the mass-gap region with $M > 2.5M_{\odot}$, but lower than the three solar masses causal limit. Another important feature of our work is that it may be possible to discriminate inflationary attractors which at the cosmological level are indistinguishable using the $M-R$ graphs of static neutron stars, however we point out the limitations in discriminating the inflationary attractors. Also we show that the WFF1, MS1 and MS1b seem to be entirely ruled out, regarding a viable description of static neutron stars. We also make the observation that as the NICER constraints are pushed towards larger radii, as for example in the case of the black widow pulsar PSR J0952-0607, it seems that equations of state that produce neutron stars with maximum masses in the mass gap region, with $M > 2.5M_{\odot}$, but lower than the three solar masses causal limit, are favored and are compatible with the modified NICER constraints. Finally we question the ability of the MPA1 equation of state to pass all the theoretical and observational constraints and we impose the question whether this equation of state plays any fundamental role in static neutron star physics.

DOI: 10.1103/PhysRevD.107.104039

I. INTRODUCTION

Direct gravitational waves observations have utterly changed the perspective of physicists on how they understand the Universe. Starting with the kilonova event GW170817 [1,2], theorists coming from cosmology and particle physics had to revise which theories can describe a realistic theory of cosmology, narrowing down significantly the available theories, since the event excluded all massive gravity theories [3–6]. Refinements to theories that predict a massive tensor spectrum were offered in the literature [7–9], however, everything in the literature now is abundantly clear which theories are cosmologically viable. Thus a single kilonova event already had a serious impact on the phenomenology of cosmological theories. It is highly anticipated from future observations of neutron stars (NSs) to see whether alternative information can be gained from gravitational systems in extreme gravitational environments. The main question is whether modified gravity [10–13] can play some fundamental role in extreme gravity environments, such as NSs and cosmology. At the moment, we only have hints and indications that this might be the case, but these hints are premature to justify a concrete definite answer to the problem. More observations are required on these issues. To date, there are two main events and observations that point in the direction of having heavy NSs, the GW190814 event [14] which points having NSs inside the mass-gap region $M > 2.5M_{\odot}$, and also the black-widow binary pulsar PSR J0952-0607 with mass

*odintsov@ice.cat
†voikonomou@gapps.auth.gr; v.k.oikonomou1979@gmail.com

$M = 2.35 \pm 0.17$ [15]. The latter does not predict a neutron star (NS) mass inside the mass-gap region, but still the NS is quite heavier that the NICER predictions of ∼2 solar masses. These are the hints that we believe nature might have some near future surprises with NSs inside the mass-gap region, for which the simple general relativistic (GR) description might not suffice. So for heavy NSs the only optimal and Occam's razor based approach is to assume that modified gravity in some form of it controls the hydrodynamic stability of the NS and drives its maximum mass to regions which are extremely unreachable by GR, even for the stiffest and not justifiable equations of state (EOSs). From these considerations, it is apparent that NSs [16–20]) and similar astrophysical compact objects have become the test bed of future gravitational and to some extent particle physics theories. These are a virtual laboratory at the sky in which high energy particle physics, particle astrophysics and cosmology theories can be tested. Obviously we live in the golden era of NSs and future illuminating observations are highly anticipated. Many distinct scientific areas can be studied in NSs, for example nuclear theories of extreme matter conditions [21–31], high energy theoretical and particle physics [32–36], studies in modified gravity of various forms, [37–46] and finally theoretical astrophysics studies [47–59]. Modified gravity can eventually play a fundamental role in NS physics, but this is still questionable. Indeed, in cosmology one of the alternative and theoretically consistent ways to describe dark energy in all the experimentally allowed values of the dark energy EOS, can be done by modified gravity in its various forms, while in the context of simple GR, one should resort to phantom scalar fields, a rather unappealing description of nature, for the moment at least. Apart from that, if the inflationary era ever existed, the GR description of inflation with a scalar field has many shortcomings, the most important being the excess of the inflaton's couplings to the Standard Model particles, which are needed for the thermalization of the Universe. In modified gravity, the instability of the inflationary attractor at the end of inflation causes oscillatory solutions to the curvature that may directly reheat the particle content of the Universe directly, without resorting to thermalization via particle interactions. Thus modified gravity in its various forms seems a viable description of nature, at least for the time being. In the literature there exists a vast stream of articles studying NSs in the context of modified gravity [40,41] and also in the context of scalar-tensor theories [60–80]. Among the many scalar-tensor theories, the inflationary theories are deemed the most important from multiple aspects, mainly though because they can generate a viable inflationary era compatible with the Planck data [81]. Here we shall consider an important class of inflationary theories, the inflationary attractors [82–120]. These theories are called attractors because although they originate for a different Jordan frame scalar field theory, they result to the same inflationary phenomenology in the Einstein frame, so essentially they are attracted to the same phenomenology in the Einstein frame. By taking also into account the constraints from inflationary theories, which essentially determine the values of the potential strength, the coefficient of the scalar potential, usually considered as a free parameter in astrophysical NS works, we construct and solve the Tolman-Oppenheimer-Volkoff (TOV) equations using a well-known Python-3 LSODA integrator. For our study we shall consider several popular and viable inflationary models, such as the universal attractors, the R^p attractors (three distinct model values), the induced inflation, the quadratic inflation, the Higgs inflation and the a-attractors (two distinct model values), and regarding the EOS we shall use nine different EOSs in order to describe the nuclear matter inside the NS. We shall use a piecewise polytropic approach [121,122] for all the EOS we will use, in which the low-density part can be one of the following EOSs: the SLy [123] which is a potential method EOS, the AP3-AP4 [124] which is a variational method EOS, the WFF1 [125] which is also a variational method EOS, the ENG [126] and the MPA1 [127] which are relativistic EOSs, the MS1 and MS1b [128] which are relativistic mean field theory EOSs, with the MS1b being identical to the MS1 with a low symmetry energy of 25 MeV and finally the APR EOS [129]. Our aim for solving the TOV equations is to obtain the masses and radii of NSs in the Jordan frame eventually, and construct the $M - R$ graphs. Regarding the gravitational mass, we shall consider the Arnowitt-Deser-Misner (ADM) masses [130] and we shall provide an explicit formula on this. We shall eventually confront our results with the observational data, using theoretical and observational constraints. Particularly, we shall consider three types of constraints, which we call CSI, CSII and CSIII. The CSI was first introduced in Ref. [47] and indicates that the radius of a $1.4M_\odot$ mass NS must be $R_{1.4M_\odot} = 12.42^{+0.52}_{-0.99}$ while the radius of a $2M_\odot$ mass NS must be $R_{2M_\odot} = 12.11^{+1.11}_{-1.23}$ km. The second constraint we shall consider is CSII and was introduced in Ref. [56] and indicates that the radius of a $1.4M_\odot$ mass NS must be $R_{1.4M_\odot} = 12.33^{+0.76}_{-0.81}$ km. Furthermore, we shall consider a third constraint, namely CSIII, which was first introduced in Ref. [51] and indicates that the radius of a $1.6M_\odot$ mass NS must be larger than $R_{1.6M_\odot} > 10.68^{+0.15}_{-0.04}$ km, while when the radius of a NS with maximum mass is considered, it must be larger than $R_{M_{\max}} > 9.6^{+0.14}_{-0.03}$ km. A graphical representation of the constraints CSI, CSII and CSIII can be found in Fig. 1.

In addition to these constraints, we shall also include the NICER I constraints [131] valid for $M = 1.4M_\odot$ NSs, which constrains the radius to be $R_{1.4M_\odot} = 11.34$–13.23 km. Furthermore, we shall also consider a theoretical refinement of the NICER constraint recently introduced in [58] by taking into account the heavy black-widow binary pulsar PSR J0952-0607 with mass $M = 2.35 \pm 0.17$ [15]. We shall call this constraint NICER II. The NICER II constrains the radius

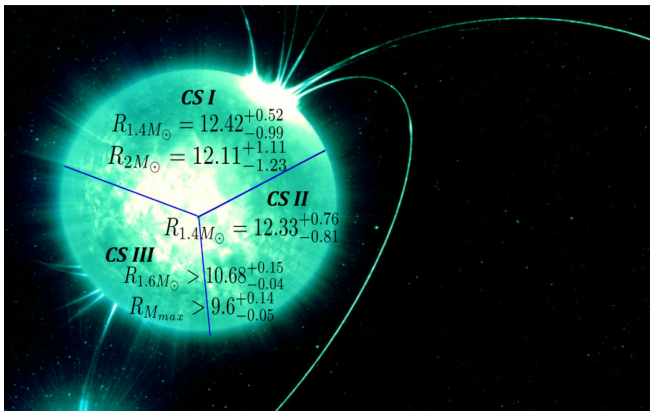

FIG. 1. An illustrative presentation of the constraints CSI [47] $R_{1.4M_\odot} = 12.42^{+0.52}_{-0.99}$ and $R_{2M_\odot} = 12.11^{+1.11}_{-1.23}$ km, the constraint CSII [56] in which case $R_{1.4M_\odot} = 12.33^{+0.76}_{-0.81}$ km and the constraint CSIII [51] in which case the radius of an $1.6M_\odot$ mass NS must be larger than $R_{1.6M_\odot} > 10.68^{+0.15}_{-0.04}$ km and for the maximum mass of a NS, the corresponding radius must be large than $R_{M_{\max}} > 9.6^{+0.14}_{-0.03}$ km. This illustrative figure is edited based on a public image of ESO, which can be found freely.[1]

of a $M = 1.4M_\odot$ to be $R_{1.4M_\odot} = 12.33$–13.25 km. After performing a thorough analysis of all the models and EOSs, we show that the MPA1 EOS, shows remarkable compatibility properties with all the constraints. We discuss in detail the phenomenological implications of our results.

II. NEUTRON STAR PHYSICS AND COSMOLOGICAL ASPECTS OF INFLATIONARY ATTRACTORS: NOTATION, FORMALISM AND EOSs

In general, there is a different notation between neutron star physics applications of nonminimally coupled scalar theories and inflationary nonminimally coupled theories. In this section we shall bridge the gap between the two distinct approaches and we shall make a direct correspondence between the notation of the two approaches. We first consider the inflationary attractors context, see [82–120]. See also Refs. [132–135] regarding the conformal transformations in inflationary theories. We first consider the Jordan frame gravitational action of a nonminimally coupled scalar field,

$$\mathcal{S}_J = \int d^4x \left[f(\phi)R - \frac{\omega(\phi)}{2} g^{\mu\nu}\partial_\mu\phi\partial_\nu\phi - U(\phi) \right] + S_m(g_{\mu\nu}, \psi_m), \tag{1}$$

where we also took into account the presence of perfect matter fluids quantified by the action $S_m(g_{\mu\nu}, \psi_m)$, and we denote the pressure of the perfect matter fluids as P while their energy density as ϵ. For cosmological applications it is customary to use natural units ($c = \hbar = 1$), while in contrast for NS applications one uses geometrized units. In the minimally coupled version of the Jordan frame case, one has the Einstein frame theory at hand, with

$$f(\phi) = \frac{1}{16\pi G} = \frac{M_p^2}{2}, \tag{2}$$

and the reduced Planck mass in natural units is defined as

$$M_p = \frac{1}{\sqrt{8\pi G}}, \tag{3}$$

with G being the Jordan frame Newton's gravitational constant. Regarding the nonminimally coupled Jordan frame theory, we perform the conformal transformation,

$$\tilde{g}_{\mu\nu} = \Omega^2 g_{\mu\nu}, \tag{4}$$

and one obtains the Einstein frame gravitational action, and we use the "tilde" to denote the Einstein frame physical quantities. In the Einstein frame, one obtains the minimally coupled scalar field theory by choosing the function Ω entering the conformal transformation as follows [132,133]:

$$\Omega^2 = \frac{2}{M_p^2} f(\phi), \tag{5}$$

therefore, by making the conformal transformation in the action (1), and by also making the choice (5), the Einstein frame action is obtained, which reads

$$\mathcal{S}_E = \int d^4x \sqrt{-\tilde{g}} \left[\frac{M_p^2}{2}\tilde{R} - \frac{\zeta(\phi)}{2}\tilde{g}^{\mu\nu}\tilde{\partial}_\mu\phi\tilde{\partial}_\nu\phi - V(\phi) \right] + S_m(\Omega^{-2}\tilde{g}_{\mu\nu}, \psi_m), \tag{6}$$

and the Einstein frame scalar field potential $V(\phi)$ is related to the corresponding Jordan frame scalar field potential $U(\phi)$ in the following way:

$$V(\phi) = \frac{U(\phi)}{\Omega^4}, \tag{7}$$

and furthermore the definition of the function $\zeta(\phi)$ is

$$\zeta(\phi) = \frac{M_p^2}{2}\left(\frac{3(\frac{df}{d\phi})^2}{f^2} + \frac{2\omega(\phi)}{f} \right). \tag{8}$$

By appropriately choosing the kinetic term of the scalar field, namely the function $\zeta(\phi)$, one can render the Einstein frame scalar theory canonical. This can be done in terms of the following transformation:

$$\left(\frac{d\varphi}{d\phi}\right) = \sqrt{\zeta(\phi)}, \tag{9}$$

[1]ESO/L.Calçada: https://www.eso.org/public/images/eso0831a/.

and thus, the Einstein frame scalar field theory acquires its well-known canonical form,

$$\mathcal{S}_E = \int d^4x\sqrt{-\tilde{g}}\left[\frac{M_p^2}{2}\tilde{R} - \frac{1}{2}\tilde{g}^{\mu\nu}\tilde{\partial}_\mu\varphi\tilde{\partial}_\nu\varphi - V(\varphi)\right] + S_m(\Omega^2\tilde{g}_{\mu\nu}, \psi_m) \tag{10}$$

with

$$V(\varphi) = \frac{U(\varphi)}{\Omega^4} = \frac{U(\varphi)}{4M_p^4 f^2}. \tag{11}$$

An important feature of the Einstein frame theory is the fact that the matter fluids are no longer perfect fluids, and the fact that can be seen by the energy momentum tensor which satisfies

$$\tilde{\partial}^\mu \tilde{T}_{\mu\nu} = -\frac{d}{d\varphi}[\ln\Omega]\tilde{T}\tilde{\partial}_\nu\phi. \tag{12}$$

Furthermore, the energy density and the pressure of the matter fluids have the following transformation properties between the Jordan and the Einstein frame:

$$\tilde{\varepsilon} = \Omega^{-4}(\varphi)\varepsilon, \qquad \tilde{P} = \Omega^{-4}(\varphi)P, \tag{13}$$

where recall that the tilde denotes Einstein frame physical quantities. A useful notation for the Einstein frame scalar field theory is the following:

$$\mathcal{S}_E = \int d^4x\sqrt{-\tilde{g}}\left[\frac{M_p^2}{2}\tilde{R} - \frac{1}{2}\tilde{g}^{\mu\nu}\tilde{\partial}_\mu\varphi\tilde{\partial}_\nu\varphi - V(\varphi)\right], \tag{14}$$

which can be further cast as follows:

$$\mathcal{S}_E = \int d^4x\sqrt{-\tilde{g}}\left[\frac{1}{16\pi G}\tilde{R} - \frac{1}{2}\tilde{g}^{\mu\nu}\tilde{\partial}_\mu\varphi\tilde{\partial}_\nu\varphi - \frac{16\pi G V(\varphi)}{16\pi G}\right], \tag{15}$$

with $M_p^2 = \frac{1}{8\pi G}$. The expression of (15) is useful for NS physics. We need to note that all these theories seen as Jordan frame theories generally violate the weak equivalence principle, see for example [136,137]. Specifically, the Jordan frame scalar theory transformed in the Einstein frame generally exactly violates the weak equivalence principle [136] unless the coupling of the scalar field to gravity in the Jordan frame is conformal. Let us note that if the scalar field disappears from the Universe due to its decays during the radiation domination era to the Standard Model particles, which is actually the mechanism of reheating in inflaton based inflationary theories, the violation of the equivalence principle has eventually disappeared from the Universe and has no effect on the Solar System experiments. Else, a fifth force should be present so in these theories the post-Newtonian parameters are affected, but to date for most scalar-tensor theories no important violation of the equivalence principle is predicted. Such strong deviations would be present for theories in which $\frac{d^2\ln A(\varphi)}{d\varphi^2} \leq -4$ [see below Eq. (20) for a definition], a constraint which does not hold true for the theories which we shall study. Caution is needed for theories in which the coupling function $A(\varphi)$ is sinusoidal. Of course all these issues could be avoided if the inflationary theory is generated geometrically via some $f(R)$ gravity, but still we should have these issues into account if one uses the conformally transformed version of the theory in the Einstein frame.

Now let us proceed to the formalism and notation of nonminimally coupled scalar field theories in the Jordan frame, customary for NS applications. We shall adopt the notation of [60] and we shall derive the TOV equations in general format for scalar field theories with potential. In theoretical astrophysics contexts it is customary to use geometrized units ($G = c = 1$), so let us express the Jordan frame gravitational action of a nonminimally coupled inflationary theory we presented previously, in a theoretical astrophysics context, which is the following:

$$\mathcal{S} = \int d^4x\frac{\sqrt{-g}}{16\pi}\left[\Omega(\phi)R - \frac{1}{2}g^{\mu\nu}\partial_\mu\phi\partial_\nu\phi - U(\phi)\right] + S_m(\psi_m, g_{\mu\nu}), \tag{16}$$

and by making the following conformal transformation,

$$\tilde{g}_{\mu\nu} = A^{-2}g_{\mu\nu}, \qquad A(\phi) = \Omega^{-1/2}(\phi), \tag{17}$$

we obtain the Einstein frame scalar field action,

$$\mathcal{S} = \int d^4x\sqrt{-\tilde{g}}\left(\frac{\tilde{R}}{16\pi} - \frac{1}{2}\tilde{g}_{\mu\nu}\partial^\mu\varphi\partial^\nu\varphi - \frac{V(\varphi)}{16\pi}\right) + S_m(\psi_m, A^2(\varphi)g_{\mu\nu}), \tag{18}$$

where φ denotes the Einstein frame canonical scalar field in the Einstein frame canonical scalar field, with its potential in the Einstein frame $V(\varphi)$ being related to the Jordan frame potential $U(\phi)$ as follows:

$$V(\varphi) = \frac{U(\phi)}{\Omega^2}. \tag{19}$$

We also define the useful function $\alpha(\varphi)$,

$$\alpha(\varphi) = \frac{d\ln A(\varphi)}{d\varphi}, \tag{20}$$

which will enter in the final expressions of the TOV equations, along with the scalar potential $V(\varphi)$ and the

function $A(\varphi) = \Omega^{-1/2}(\phi)$. For the description of spacetime around and in static NSs, we shall use the following spherically symmetric metric:

$$ds^2 = -e^{\nu(r)}dt^2 + \frac{dr^2}{1-\frac{2m(r)}{r}} + r^2(d\theta^2 + \sin^2\theta d\phi^2), \quad (21)$$

where the function $m(r)$ describes the NS gravitational mass and r denotes the circumferential radius. One of the aims of solving the TOV equations is to determine in a numerical way the two functions $\nu(r)$ and $\frac{1}{1-\frac{2m(r)}{r}}$. Let us describe in brief the physics of the NS for the scalar-tensor theory at hand. The metric function $\nu(r)$ has a nonzero value at the center of the NS, and beyond the NS surface, contrary to the GR case, the metric is no longer matched to the Schwarzschild metric, because the functions $\nu(r)$ and $m(r)$ have additional contributions from the scalar field. Thus in the present case, the matching of the spherically symmetric metric (21) with the Schwarzschild metric will only be performed at numerical infinity. The latter will be appropriately determined during the numerical manipulation of the TOV equations, by checking which values of the radial parameter r optimize the scalar field solutions at large distance beyond the surface of the star. The TOV equations for the Einstein frame scalar field theory for the metric spherically symmetric metric (21) take the following form:

$$\frac{dm}{dr} = 4\pi r^2 A^4(\varphi)\varepsilon + \frac{r}{2}(r-2m(r))\omega^2 + 4\pi r^2 V(\varphi), \quad (22)$$

$$\frac{d\nu}{dr} = r\omega^2 + \frac{2}{r(r-2m(r))}\left[4\pi A^4(\varphi)r^3 P - 4\pi V(\varphi)r^3\right] + \frac{2m(r)}{r(r-2m(r))}, \quad (23)$$

$$\frac{d\omega}{dr} = \frac{4\pi r A^4(\varphi)}{r-2m(r)}\Big(\alpha(\varphi)(\epsilon-3P) + r\omega(\epsilon-P)\Big) - \frac{2\omega(r-m(r))}{r(r-2m(r))} + \frac{8\pi\omega r^2 V(\varphi) + r\frac{dV(\varphi)}{d\varphi}}{r-2m(r)}, \quad (24)$$

$$\frac{dP}{dr} = -(\epsilon+P)\left[\frac{1}{2}\frac{d\nu}{dr} + \alpha(\varphi)\omega\right], \quad (25)$$

$$\omega = \frac{d\varphi}{dr}, \quad (26)$$

where the definition of the function $\alpha(\varphi)$ is given in Eq. (20). Also the pressure and the energy density P and ϵ denote Jordan frame quantities, and we shall keep these until the end of the calculations. Now for the solution of the TOV equations, we need to solve these numerically for the interior and the exterior of the NS, independently, and we shall solve the following initial conditions:

$$P(0) = P_c, \qquad m(0) = 0, \qquad \nu(0) = -\nu_c,$$
$$\varphi(0) = \varphi_c, \qquad \omega(0) = 0. \quad (27)$$

Note that the values ν_c and φ_c are initially arbitrary and their exact correct value will be determined by using a double shooting method which will determine which values ν_c and φ_c yield the correct behavior of the scalar field at numerical infinity.

Regarding the EOS, we shall use nine distinct EOSs in order to describe the nuclear matter inside the NS. We shall adopt a piecewise polytropic approach [121,122] for all the EOSs, in which the low-density part can be one of the following EOSs: the SLy [123] which is a potential method EOS, the AP3-AP4 [124] which is a variational method EOS, the WFF1 [125] which is also a variational method EOS, the ENG [126] and the MPA1 [127] which are relativistic EOSs, the MS1 and MS1b [128] which are relativistic mean field theory EOSs, with the MS1b being identical to the MS1 with a low symmetry energy of 25 MeV and finally the APR EOS [129]. As we shall demonstrate, the MPA1 EOS leads to remarkable results regarding the compatibility of all the attractor models with all the constraints. The MPA1 is a relativistic EOS based on relativistic Brueckner-Hartree-Fock calculations. We need to note that all the EOSs we mentioned above and which we shall consider, lead to a subluminal maximum speed of sound speed, save for the WFF1. But as we will show, the WFF1 is excluded for most of the models, when the observational data are confronted.

The use of a piecewise polytropic EOS is highly motivated by our lack of knowledge of the actual relation between the pressure and the baryon mass density beyond the nuclear density and, moreover, it is still uncertain of what matter is composed of in the core of NS. What we know though is that the Fermi energy of the matter particles that compose the NSs is much higher than the temperature of NSs. The piecewise polytropic EOS is constructed by using phenomenological data on nuclear matter, this is why it is considered to be a complete EOS. In principle, the NSs temperature is much lower compared to the Fermi energy of the particles that constitute NSs, thus in general NS matter can be described by a single-parameter polytropic EOS that may accurately describe cold matter when densities higher than the nuclear density are considered. However, the uncertainty of the EOS problem always emerges, which is of course higher as the NS central density is increased. The pressure considered as a function of the NS baryonic mass density is in general ill defined and it is unknown to at least 1 order of magnitude, when densities above the nuclear density are considered. In addition to this issue, the actual nature of the matter phase at the core of NS is unknown; is it made of quarks, hyperons? Nobody can

answer these questions rigorously. Thus, by using a parametrized EOS engineered to function at high densities can serve as an optimal scientific choice for the description of the EOS of NSs. The piecewise polytropic EOS is exactly this type of EOS. For the construction of the piecewise polytropic EOS, theoretical and observational astrophysical constraints are considered, including the very important causality constraint [121,122]. The piecewise polytropic EOS is constructed by using a low density part with density ρ satisfying $\rho < \rho_0$ with ρ_0 being the nuclear saturation density, and by construction a well-known tabulated EOS is used, like the SLy or other EOSs. Also a large density part composes the piecewise polytropic EOS. In fact, the actual differences between the NS physical quantities, like the Jordan frame mass and radius, using the piecewise polytropic EOSs and their ordinary counterparts is of the order $\mathcal{O}(0.1)\%$ in the context of GR, but still the piecewise polytropic equation of state approach is more complete from a phenomenological standpoint for the reasons we discussed above. We need to note though that there exist studies in the literature that, for medium or low-mass neutron stars, the error of piecewise polytropic EOSs with ordinary polytropic EOSs can be of the order $\sim\mathcal{O}(10\%)$ for the Jordan frame mass M and of the order $\sim\mathcal{O}(2\%)$ for the Jordan frame radius R [138]. Also alternative spectral EOS studies exist [139] which do not yield high errors at lower masses. Later on we shall present a table in which we shall compare the Jordan frame masses and radii of NSs with polytropic and piecewise polytropic EOSs choosing the MPA1 EOS.

In order to maintain the article self-contained, we shall briefly describe the piecewise polytropic EOS, which is constructed by using a low-density part describing the crust, with $\rho < \rho_0$, and ρ_0 being obtained by matching the high density part with the low-density part. The piecewise polytropic EOS also contains two high densities $\rho_1 = 10^{14.7}$ g/cm^3 and $\rho_2 = 10^{15.0}$ g/cm^3, and the intermediate pressures and densities $\rho_{i-1} \leq \rho \leq \rho_i$ satisfy the following relation:

$$P = K_i \rho^{\Gamma_i}. \tag{28}$$

Also we need to require the continuity constraint in each intermediate patch of the piecewise polytropic EOS,

$$P(\rho_i) = K_i \rho^{\Gamma_i} = K_{i+1} \rho^{\Gamma_{i+1}}. \tag{29}$$

From the continuity constraint, by employing Eq. (29) the parameters K_2 and K_3 are derived, given the parameters K_1, Γ_1, Γ_2, Γ_3, which are basically determined by the low-density part EOS. Each distinct EOS has a different set of parameters K_1 (or equivalently an initial pressure p_1), Γ_1, Γ_2, and Γ_3. The energy density of the piecewise polytropic EOS as a function of the pressure can be obtained by using

$$d\frac{\epsilon}{\rho} = -P d\frac{1}{\rho}, \tag{30}$$

considering always a barotropic fluid, and due to the continuity equation we get

$$\epsilon(\rho) = (1+\alpha_i)\rho + \frac{K_i}{\Gamma_i - 1}\rho^{\Gamma_i}, \tag{31}$$

which is valid for $\Gamma_i \neq 1$, and furthermore the parameter α_i is

$$\alpha_i = \frac{\epsilon(\rho_{i-1})}{\rho_{i-1}} - 1 - \frac{K_i}{\Gamma_i - 1}\rho_{i-1}^{\Gamma_i - 1}. \tag{32}$$

Having discussed the EOSs we shall use, now let us focus on the gravitational mass of the static NSs, which is essentially what we shall calculate numerically when we shall solve the TOV equations. We shall consider the ADM mass, and the solution of the TOV equations shall yield the Einstein frame ADM mass, but in the end we shall transform it to the Jordan frame counterpart. The Jordan frame ADM is basically what is relevant for weak field approximation Keplerian orbits. Let us present the Jordan frame ADM mass expressed in terms of the Einstein frame mass, so let us introduce K_E and K_J which in geometrized units are defined as follows:

$$\mathcal{K}_E = 1 - \frac{2m}{r_E}, \tag{33}$$

$$\mathcal{K}_J = 1 - \frac{2m_J}{r_J}. \tag{34}$$

The quantities $\mathcal{K}_E$ and $\mathcal{K}_J$ are related as follows:

$$\mathcal{K}_J = A^{-2}\mathcal{K}_E, \tag{35}$$

and the radii of the NSs in the Jordan and Einstein frames are related as follows:

$$r_J = A r_E, \tag{36}$$

and the ADM mass of the NS in the Jordan frame is defined as follows:

$$M_J = \lim_{r\to\infty} \frac{r_J}{2}(1 - \mathcal{K}_J), \tag{37}$$

and the Einstein frame counterpart is

$$M_E = \lim_{r\to\infty} \frac{r_E}{2}(1 - \mathcal{K}_E). \tag{38}$$

By taking the asymptotic limit of Eq. (35), we get the following formula:

$$\mathcal{K}_J(r_E) = \left(1 + \alpha(\varphi(r_E))\frac{d\varphi}{dr}r_E\right)^2 \mathcal{K}_E(\varphi(r_E)), \quad (39)$$

where r_E denotes the Einstein frame radius at distances far away from the surface of the NS, and furthermore $\frac{d\varphi}{dr} = \frac{d\varphi}{dr}|_{r=r_E}$. Using Eqs. (34)–(39) we obtain the final relation of the Jordan frame ADM mass,

$$M_J = A(\varphi(r_E))\left(M_E - \frac{r_E^2}{2}\alpha(\varphi(r_E))\frac{d\varphi}{dr} \times \left(2 + \alpha(\varphi(r_E))r_E\frac{d\varphi}{dr}\right)\left(1 - \frac{2M_E}{r_E}\right)\right), \quad (40)$$

where recall that $\frac{d\varphi}{dr} = \frac{d\varphi}{dr}|_{r=r_E}$. Hereafter we shall denote the Jordan frame ADM mass M_J as $M = M_J$ and the central part of our calculation will be the determination of this mass given in Eq. (40). Regarding the radius of the neutron star, we need to evaluate the Jordan frame one R from the Einstein frame one R_s, which are related by

$$R = A(\varphi(R_s))R_s, \quad (41)$$

and the Einstein frame NS mass is determined by $P(R_s) = 0$. In the following we shall numerically calculate the Jordan frame masses and the radii of the NS for several inflationary attractor potentials and we shall construct the $M - R$ graphs. In the following subsections we shall present in brief the inflationary models we shall consider in this article.

A. Inflation and NSs physics with a attractors

The a attractors [82–120] are perhaps the most popular class of inflationary models, because most of the well-known inflationary models compatible with the latest Planck data [81] fall under this category. These models produce identical observational indices of inflation with the Starobinsky model and with the Higgs inflation, although they originate from distinct Jordan frame theories. The analysis of NSs physics for some EOSs, which will be studied in this work, can be found in Ref. [74]. Using the notation of the previous sections, the a attractors correspond to the following choice of the kinetic term in the Jordan frame,

$$\omega(\phi) = \frac{1}{4\xi}\frac{1}{f}\left(\frac{df}{d\phi}\right)^2, \quad (42)$$

and furthermore the scalar field potential in the Jordan frame is

$$U(\phi) = \mathcal{U}_0 f^2\left(1 - \frac{1}{f}\right)^{2n}. \quad (43)$$

Then we get

$$\frac{d\varphi}{d\phi} = \sqrt{\frac{3a}{16\pi}}\frac{1}{f}\left(\frac{df}{d\phi}\right), \quad (44)$$

where a is equal to

$$a = 1 + \frac{1}{6\xi}. \quad (45)$$

Upon integration of Eq. (44) we obtain

$$f = e^{\sqrt{\frac{16\pi}{3a}}\varphi}, \quad (46)$$

which remarkably holds true irrespectively of the actual form of the function f. The Jordan and Einstein frame potentials are related by

$$V(\varphi) = \frac{U(\phi)}{f^2}, \quad (47)$$

thus from Eqs. (43) and (46), the Einstein frame scalar field potential is obtained,

$$V(\varphi) = \mathcal{U}_0(1 - e^{-\sqrt{\frac{16\pi}{3a}}\varphi})^{2n}, \quad (48)$$

and we shall use the above for NS physics for the a-attractor models, in geometrized units. The conformal factor $A(\phi)$ in terms of φ reads

$$A(\varphi) = e^{\alpha\varphi}, \quad (49)$$

with α in the case at hand being

$$\alpha = -\frac{1}{2}\sqrt{\frac{16\pi}{3a}}, \quad (50)$$

and therefore the function $\alpha(\varphi)$ defined in Eq. (20) reads, hence in the case at hand,

$$a(\varphi) = \alpha = -\frac{1}{2}\sqrt{\frac{16\pi}{3a}}, \quad (51)$$

and accordingly, the Einstein frame scalar field potential in terms of the parameter α reads

$$V(\varphi) = \mathcal{U}_0(1 - e^{2\alpha\varphi})^{2n}, \quad (52)$$

which will be used for solving the TOV equations later on. One important feature of inflationary theories, when studying NSs, usually not taken into account in the existing literature, is the fact that the values of $\mathcal{U}_0$ are not freely

chosen, but these are constrained by the inflationary theories. The correct value of $\mathcal{U}_0$ which must be taken into account can be found by directly matching the inflationary theory with the corresponding one in geometrized units, used in NS physics. Then we get that $\mathcal{U}_0$ appearing in Eq. (52) is $\mathcal{U}_0 = 16\pi\mathcal{V}_0$. Now $\mathcal{V}_0$ is severely constrained by the inflationary theory, so let us develop the inflationary theory and thereafter we shall obtain the actual value of $\mathcal{U}_0$ to be used in the numerical study of the TOV equations. The a attractors have the following Jordan frame inflationary potential in natural units:

$$U(\phi) = V_0 f^2 \left(1 - \frac{1}{f}\right)^{2n}, \tag{53}$$

and the corresponding Einstein frame scalar potential is

$$V(\varphi) = \mathcal{V}_0 \left(1 - \frac{1}{f}\right)^{2n} = \tilde{V}_0 M_p^4 \left(1 - \frac{1}{f}\right)^{2n}, \tag{54}$$

with $\mathcal{V}_0 = \tilde{V}_0 M_p^4$ in natural units, and also $\tilde{V}_0 = \frac{V_0}{4}$, therefore $\tilde{V}_0$ is essentially dimensionless in natural units and furthermore $\mathcal{V}_0$ has mass dimensions $[m]^4$. The scalar potentials of the form (53) are widely known as E-model potentials, and for $n = 2$ one obtains the a-attractor potentials. For all the values that the parameter a can take, the a attractors and E models remarkably yield the same observational indices of inflation, namely the same scalar spectral index n_s and the same tensor-to-scalar ratio r [85]. For our analysis we shall be interested in values $a \sim \mathcal{O}(10)$ and also we shall consider values of the order $a \sim \mathcal{O}(10^4)$, and the inflationary theory is still viable. For small values of a, the observational indices acquire the following form at leading order in terms of the e-foldings number N:

$$n_s \simeq 1 - \frac{2}{N}, \qquad r = \frac{12a}{N^2}, \tag{55}$$

while for large values of a ($a \gg \frac{8N}{3}$), the observational indices take the form [85]

$$n_s = 1 - \frac{2}{N}, \qquad r = \frac{8}{N}. \tag{56}$$

Now let us demonstrate the allowed values of $\tilde{V}_0$ given in Eq. (54), which eventually will determine the allowed values of $\mathcal{U}_0$ given in (52). The actual values of $\tilde{V}_0$ are constrained by the amplitude of the scalar perturbations for a minimally coupled scalar field, denoted as Δ_s^2, which is defined to be

$$\Delta_s^2 = \frac{1}{24\pi^2} \frac{V(\varphi_f)}{M_p^4} \frac{1}{\epsilon(\varphi_f)}, \tag{57}$$

the values of which are constrained to be [81]

$$\Delta_s^2 = 2.2 \times 10^{-9}, \tag{58}$$

where φ_f denotes the scalar field value at the end of the inflationary era, and furthermore ϵ denotes the first slow-roll index of inflation. For the case at hand,

$$\mathcal{V}_0 = \tilde{V}_0 M_p^4 \sim 9.6 \times 10^{-11} M_p^4. \tag{59}$$

Thus, in view of the fact that $M_p = 1/\sqrt{8\pi}$ in geometrized units, we have for $\mathcal{U}_0$,

$$\mathcal{U}_0 = 7.62094 \times 10^{-12}. \tag{60}$$

This is the actual value of $\mathcal{U}_0$ which we shall use in geometrized units.

B. Inflation and NS physics with quadratic and induced inflation attractors

Now let us consider another mainstream class of inflationary attractor potentials, namely the quadratic and induced inflation attractors class which again belong to a wider class of attractors [82–120]. These models in the Einstein frame lead to the same minimally coupled scalar field theory, with similar inflationary properties, although originating from distinct nonminimally coupled Jordan frame theories. The analysis of NSs in this kind of theories, for some of the EOSs used in this article, can be found in Ref. [140]. For both models, the Jordan frame nonminimally coupled theory is

$$\mathcal{S}_J = \int d^4x\sqrt{-g}\left[\Omega(\phi)R - \frac{1}{2}g^{\mu\nu}\partial_\mu\phi\partial_\nu\phi - U(\phi)\right] + S_m(g_{\mu\nu}, \psi_m), \tag{61}$$

and note that in the case of induced inflation and quadratic attractors, the kinetic term of the scalar field in the Jordan frame is canonical. The Jordan frame functions $\Omega(\phi)$ and $U(\phi)$ have the form [82]

$$\Omega(\phi) = (1 + \xi f(\phi)), \quad U(\phi) = M_p^4 \lambda (\Omega(\phi) - 1)^2. \tag{62}$$

The free parameters λ, ξ and the nonminimal coupling function $f(\phi)$ have no mass dimensions in natural units. The values of the parameter ξ, to which we shall refer to as nonminimal coupling, at strong and weak coupling limit yield the two distinct models, the induced inflation and the quadratic attractors. The strong coupling theory $\xi \gg 1$ corresponds to the induced inflation theory, while the weak coupling theory $\xi \ll 1$ yields the quadratic attractors. For the induced inflation attractors, the nonminimal coupling function $\Omega(\phi)$ and the scalar field potential are

$$\Omega(\phi) = \xi f(\phi), \qquad U(\phi) = \lambda M_p^4 \xi^2 f(\phi)^2. \tag{63}$$

The Einstein frame scalar field potential $V(\varphi)$ is

$$V(\varphi) = V_s\left(1 - e^{-\sqrt{\frac{2}{3}}\frac{\varphi}{M_p}}\right)^2, \tag{64}$$

with $V_s = \frac{M_p^4 \lambda}{\xi^2}$, which is constrained to be

$$V_s \sim 9.6 \times 10^{-11} M_p^4, \tag{65}$$

and in effect, the free parameters λ and ξ of the induced inflation are chosen so that $\frac{\lambda}{\xi^2} \sim 10^{-11}$, hence for $\xi \sim 10^5$ and for $\lambda \sim 1$ a viable inflationary era is produced. Furthermore, the nonminimal coupling function $\Omega(\varphi)$ is

$$\Omega(\varphi) = e^{\sqrt{\frac{2}{3}}\frac{\varphi}{M_p}}. \tag{66}$$

The observational indices for inflation at leading order in terms of the e-foldings number read

$$n_s = 1 - \frac{2}{N}, \qquad r = \frac{12}{N^2}. \tag{67}$$

As it can be seen, the inflationary phenomenology of the induced inflation attractors is indistinguishable from the Starobinsky and Higgs inflation model. It is notable that for the induced inflation attractors, one does not even need to define the functional form of the Jordan frame function $f(\phi)$.

Regarding the quadratic attractors, the weak coupling limit of the same Jordan frame theory, the function $\Omega(\varphi)$ and the Einstein frame scalar potential are at leading order [82],

$$\Omega(\varphi) = \xi\left(\xi^{-1} + \frac{g_1}{M_p}\varphi\right), \qquad V(\varphi) = \lambda \frac{g_1^2}{M_p^2}\varphi^2, \tag{68}$$

where $g_1 \ll \xi^{-1}$, and g_1 denotes the expansion parameter. For the quadratic attractors, the observational indices of inflation at leading order in the e-foldings number N take the form

$$n_s = 1 - \frac{2}{N}, \qquad r = \frac{8}{N}, \tag{69}$$

and note that this result does not depend on the functional form of $f(\phi)$. From the Einstein frame potential, due to the constraints on the amplitude of the scalar perturbations, the parameter λ must satisfy $\lambda g_1^2 \sim 10^{-11}$ and we can easily satisfy this by using $\lambda \sim \mathcal{O}(1)$ and $g_1 \sim \mathcal{O}(10^{-5})$, while the parameter ξ can be chosen to be $\xi \sim 10^{-2}$.

Regarding the NSs analysis, for the induced inflation we have

$$A(\varphi) = e^{-\frac{1}{2}\sqrt{\frac{2}{3}}\varphi}, \tag{70}$$

and $\alpha(\phi)$ is

$$a(\varphi) = -\frac{1}{2}\sqrt{\frac{2}{3}}, \tag{71}$$

while the scalar potential in the Einstein frame is

$$V(\varphi) = V_s\left(1 - e^{-\sqrt{\frac{2}{3}}\varphi}\right)^2. \tag{72}$$

Regarding the quadratic attractors, the Einstein frame scalar potential is

$$V(\varphi) = \lambda g_1^2 \varphi^2, \tag{73}$$

and $A(\varphi)$ is

$$A(\varphi) = (1 + \xi g_1 \varphi)^{-1/2}, \tag{74}$$

while $\alpha(\varphi)$ is

$$a(\varphi) = -\frac{1}{2}\frac{\xi g_1}{1 + \xi g_1 \varphi}. \tag{75}$$

Let us recapitulate the values of the free parameters for the two inflationary attractors, and for the induced inflation case, we must choose $\xi \sim \mathcal{O}(10^5)$, $\lambda \sim \mathcal{O}(1)$ while for the quadratic attractors we choose $\xi \sim \mathcal{O}(10^{-2})$, $\lambda \sim \mathcal{O}(1)$ and $g_1 \sim \mathcal{O}(10^{-4})$. Usually, in the astrophysics literature, these parameters would be chosen freely, but these are not free parameters and are severely constrained by the corresponding inflationary theories.

C. Inflation and NSs physics with R^p attractors

The R^p attractors is a special class of inflationary attractors which were developed in Ref. [141], and are based on the following Einstein frame scalar potential:

$$V(\varphi) = V_0 M_p^4 e^{-2\sqrt{\frac{2}{3}}\kappa\varphi}\left(e^{\sqrt{\frac{2}{3}}\kappa\varphi} - 1\right)^{\frac{p}{p-1}}. \tag{76}$$

In the Jordan frame, the R^p attractors correspond to the following $F(R)$ gravity:

$$F(R) = R + \beta R^p, \tag{77}$$

with β being a free parameter with mass dimensions $[\beta] = [m]^{2-2p}$ in natural units. The analysis of NSs in this kind of theories, for some of the EOSs used in this article, can be found in Ref. [80]. The terminology attractors for the R^p attractors is justified when considering the Jordan frame nonminimally coupled theory that these originate from. The action in the Jordan frame of such nonminimally coupled scalar theory is

$$\mathcal{S}_J = \int d^4x \left(\frac{\Omega(\phi)}{2\kappa^2}R - \frac{\omega(\phi)}{2}g^{\mu\nu}\partial_\mu\phi\partial_\nu\phi - V_J(\phi)\right), \tag{78}$$

with the coupling function having the general form $\Omega(\phi) = 1 + \xi f(\phi)$ and ξ, $f(\phi)$ are arbitrary dimensionless coupling and dimensionless function respectively. The

Jordan frame scalar theory of the R^p attractors correspond to the following scalar field potential:

$$V_J(\phi) = V_0(\Omega(\phi) - 1)^{\frac{p}{p-1}}, \tag{79}$$

and the kinetic term $\omega(\phi)$ is

$$\omega(\phi) = \frac{1}{4\xi}\frac{(\frac{d\Omega(\phi)}{d\phi})^2}{\Omega(\phi)}. \tag{80}$$

Thus the terminology attractors are justified, since multiple theories with arbitrary functions $f(\phi)$ correspond to the same scalar theory in the Einstein frame, with action

$$\mathcal{S}_E = \sqrt{-\tilde{g}}\left(\frac{\tilde{R}}{2\kappa^2} - \tilde{g}^{\mu\nu}\partial_\mu\varphi\partial_\nu\varphi - V(\varphi)\right). \tag{81}$$

The scalar potentials in the Jordan and Einstein frames are related in the following way:

$$V(\varphi) = \Omega^{-2}(\phi)V_J(\phi). \tag{82}$$

Note that the general relation between the Jordan and Einstein frame scalar fields is

$$\left(\frac{d\varphi}{d\phi}\right)^2 = \frac{3}{2}\frac{(\frac{d\Omega(\phi)}{d\phi})^2}{\Omega(\phi)} + \frac{\omega(\phi)}{\Omega(\phi)}, \tag{83}$$

therefore, for the R^p attractors case, with the kinetic term function $\omega(\phi)$ being given in Eq. (80), we have

$$\Omega(\phi) = e^{\sqrt{\frac{2}{3\alpha}}\varphi}, \tag{84}$$

where α is

$$\alpha = 1 + \frac{1}{6\xi}. \tag{85}$$

Upon substitution of Eq. (84) in Eq. (82) we get the R^p-attractor potential. Moreover, the phenomenologically important case $\alpha = 1$ is obtained when $\xi \to \infty$, or analogously when $\Omega(\phi) \ll \frac{3}{2}\frac{(\frac{d\Omega(\phi)}{d\phi})^2}{\omega(\phi)}$. The R^p attractor theories result to a viable inflationary phenomenology [141], with the observational indices of inflation being

$$n_s = \frac{(3\alpha + (3\alpha-2)p^2 + (8-6\alpha)p - 8)e^{2\sqrt{\frac{2}{3}}\sqrt{\frac{1}{\alpha}}\kappa\varphi} - 2(p-1)(-3\alpha + (3\alpha-2)p + 8)e^{\sqrt{\frac{2}{3}}\sqrt{\frac{1}{\alpha}}\kappa\varphi} + (3\alpha-8)(p-1)^2}{3\alpha(p-1)^2(e^{\sqrt{\frac{2}{3}}\sqrt{\frac{1}{\alpha}}\kappa\varphi} - 1)^2}, \tag{86}$$

$$r = \frac{16((p-2)e^{\sqrt{\frac{2}{3}}\sqrt{\frac{1}{\alpha}}\kappa\varphi} - 2p + 2)^2}{3\alpha(p-1)^2(e^{\sqrt{\frac{2}{3}}\sqrt{\frac{1}{\alpha}}\kappa\varphi} - 1)^2}, \tag{87}$$

and the parameter V_0 in the potential is constrained as follows:

$$V_0 \sim 9.6 \times 10^{-11}. \tag{88}$$

In this article, we shall consider two limiting cases of α, namely $\alpha \sim 0.1$ and $\alpha = 10^8$, with the latter covering the strong coupling limit of the theory. Also the parameter p will be assumed to take values in $1.91 \leq p \leq 1.99$, which are the most relevant for NS studies, see Ref. [80] for details. Let us present the relevant functions for the TOV equations study; the function $A(\varphi)$ for the R^p attractors is

$$A(\varphi) = e^{-\frac{1}{2}\sqrt{\frac{2}{3\alpha}}\varphi}, \tag{89}$$

hence $\alpha(\phi)$ reads

$$a(\varphi) = -\frac{1}{2}\sqrt{\frac{2}{3\alpha}}. \tag{90}$$

In addition, the Einstein frame scalar potential is

$$V(\varphi) = V_0 e^{-2\sqrt{\frac{2}{3\alpha}}\varphi}(e^{\sqrt{\frac{2}{3\alpha}}\varphi} - 1)^{\frac{p}{p-1}}, \tag{91}$$

and expressed in geometrized units, the V_0 constraint is

$$V_0 \simeq 7.62 \times 10^{-12}. \tag{92}$$

D. Inflation and NS physics with Higgs model

The Higgs inflation scalar model is very popular in cosmological contexts [142], and the NSs study in this kind of inflationary potentials was developed in Ref. [75]. The Jordan frame action for the Higgs model is

$$\mathcal{S} = \int d^4x\frac{\sqrt{-g}}{16\pi}\left[f(\phi)R - \frac{1}{2}g^{\mu\nu}\partial_\mu\phi\partial_\nu\phi - U(\phi)\right] + S_m(\psi_m, g_{\mu\nu}), \tag{93}$$

where $f(\phi)$ and $U(\phi)$ for the Higgs model are

$$f(\phi) = 1 + \xi\phi^2, \tag{94}$$

$$U(\phi) = \lambda\phi^4. \tag{95}$$

For the Higgs model, the function $A(\phi)$ is

$$A(\phi) = f^{-1/2}(\phi), \tag{96}$$

and in view of Eq. (94) we get

$$A(\phi) = (1 + \xi\phi^2)^{-1/2}. \tag{97}$$

The scalar potential reads

$$V(\phi) = \frac{U(\phi)}{f^2(\phi)}, \tag{98}$$

and expressed in terms of ϕ we have

$$V(\phi) = \frac{\lambda\phi^4}{(1 + \xi\phi^2)^2}. \tag{99}$$

The Higgs model in cosmological contexts is obtained for

$$\xi^2\phi^2 \gg 1, \tag{100}$$

and at the same time when

$$\xi^2\phi^2 \gg \xi\phi^2, \tag{101}$$

with Eq. (101) being valid for $\xi \gg 1$. Then we get

$$\frac{d\varphi}{d\phi} \simeq \frac{\sqrt{12}}{\sqrt{16\pi}}\frac{\xi\phi}{1 + \xi\phi^2} = \frac{\sqrt{12}}{2\sqrt{16\pi}}\frac{f'(\phi)}{f(\phi)}, \tag{102}$$

and by integrating, Eq. (102) the φ and ϕ relation is obtained,

$$\varphi = \frac{\sqrt{12}}{2\sqrt{16\pi}}\ln\left(f(\phi)\right) = \frac{\sqrt{12}}{2\sqrt{16\pi}}\ln\left(1 + \xi\phi^2\right), \tag{103}$$

therefore,

$$1 + \xi\phi^2 = e^{\frac{2\sqrt{16\pi}}{\sqrt{12}}\varphi}. \tag{104}$$

Thus by using Eq. (97), the function $A(\phi)$ can be expressed in terms of φ,

$$A(\varphi) = e^{\alpha\varphi}, \tag{105}$$

with α being

$$\alpha = -2\sqrt{\frac{\pi}{3}}, \tag{106}$$

and furthermore,

$$a(\varphi) = \alpha = -2\sqrt{\frac{\pi}{3}}. \tag{107}$$

Finally, the Einstein frame Higgs potential is

$$V'(\varphi) \simeq \frac{4\alpha\lambda}{\xi^2}e^{2\alpha\varphi}(e^{2\alpha\varphi} - 1). \tag{108}$$

The constraints on the scalar amplitude of curvature perturbations are in the Higgs model the following:

$$\frac{\lambda M_p^4}{4\xi^2} \sim 9.6 \times 10^{-11} M_p^4, \tag{109}$$

and in geometrized units we have

$$\frac{\lambda}{\xi^2} \sim 16\pi \times (1.51982 \times 10^{-13}), \tag{110}$$

therefore for $\lambda = 0.1$ we have $\xi \sim 11.455 \times 10^4$.

E. Inflation and NS physics with universal attractors

The NSs study of universal attractor potentials was developed in Ref. [76], and in this case, the function $f(\phi)$ has the form

$$f(\phi) = \frac{M_p^2}{2}(1 - \xi\phi^2), \tag{111}$$

with ξ being a positive coupling. The Jordan frame scalar potential is

$$U(\phi) = U_0 f^2(\phi)\left(\frac{\phi}{M_p}\right)^{2n}, \tag{112}$$

where $n > 0$. For the universal attractors we have

$$\Omega^2 = \frac{2}{M_p^2}f(\phi), \tag{113}$$

and the Einstein frame action is

$$\mathcal{S}_E = \int d^4x\sqrt{-\tilde{g}}\left[\frac{M_p^2}{2}\tilde{R} - \frac{\zeta(\phi)}{2}\tilde{g}^{\mu\nu}\tilde{\partial}_\mu\phi\tilde{\partial}_\nu\phi - V(\phi)\right] + S_m(\Omega^{-2}\tilde{g}_{\mu\nu}, \psi_m), \tag{114}$$

with

$$\zeta(\phi) = \frac{M_p^2}{2}\left(\frac{3(\frac{df}{d\phi})^2}{f^2} + \frac{2\omega(\phi)}{f}\right), \tag{115}$$

while the potentials in the two frames are related as follows:

$$V(\phi) = \frac{U(\phi)}{\Omega^4}, \tag{116}$$

with

$$V(\phi) = \frac{U_0 M_p^4}{4}\left(\frac{\phi}{M_p}\right)^{2n}. \tag{117}$$

In the case of universal attractors, the observational indices of inflation are, again,

$$n_s = 1 - \frac{2}{N}, \qquad r = \frac{12}{N^2}, \tag{118}$$

just like in the Higgs inflation and several other attractors cases.

For the universal attractor models, it is assumed that

$$\Omega(\phi) \ll \frac{3M_p^2}{2}\Omega'(\phi), \tag{119}$$

and this can be written as follows:

$$1 - \frac{\xi\phi^2}{M_p^2} \ll \frac{6\xi^2\phi^2}{M_p^2}. \tag{120}$$

Using

$$\frac{d\varphi}{d\phi} = \frac{\sqrt{1 + \frac{\xi\phi^2}{M_p^2} + \frac{6\xi^2\phi^2}{M_p^2}}}{1 + \frac{\xi\phi^2}{M_p^2}}, \tag{121}$$

and also Eq. (119), we get

$$\varphi = -\sqrt{\frac{3}{2}} M_p \ln\left(1 - \frac{\xi\phi^2}{M_p^2}\right), \tag{122}$$

which can be rewritten,

$$\frac{\phi^2}{M_p^2} = \frac{1 - e^{-\sqrt{\frac{2}{3}}\frac{\varphi}{M_p}}}{\xi}. \tag{123}$$

Thus the Einstein frame scalar potential has the final form in terms of φ,

$$V(\varphi) = \frac{U_0 M_p^4}{4\xi^n}\left(1 - e^{-\sqrt{\frac{2}{3}}\frac{\varphi}{M_p}}\right)^n, \tag{124}$$

and by setting $V_0 = \frac{U_0 M_p^4}{4\xi^n}$, due to the inflationary constraints on the amplitude of scalar perturbations, V_0 is constrained,

$$V_0 \sim 9.6 \times 10^{-11} M_p^4, \tag{125}$$

which constrains in effect the parameter ξ to be $\xi = 36.2239 \times 10^4$. Now regarding the functions that enter in the TOV equations for the universal attractors case, we have, for $A(\varphi)$,

$$A(\varphi) = e^{2\sqrt{\frac{\pi}{3}}\varphi}, \tag{126}$$

while $a(\varphi)$ reads

$$a(\varphi) = \alpha = 2\sqrt{\frac{\pi}{3}}. \tag{127}$$

F. Results and confrontation with the data

Let us now present the results of our numerical analysis we performed using the LSODA technique for solving the TOV equations. We analyzed all the inflationary attractors we mentioned in the previous sections, namely, the a attractors for two characteristic values of the free parameters, the R^p attractors for three characteristic values of the free parameters, the universal attractors, the quadratic attractors, the Higgs and induced inflation cases. We used the following EOSs, as we mentioned earlier: the SLy [123] which is a potential method EOS, the AP3-AP4 [124] which is a variational method EOS, the WFF1 [125] which is also a variational method EOS, the ENG [126] and the MPA1 [127] which are relativistic EOSs, the MS1 and MS1b [128] which are relativistic mean field theory EOSs, with the MS1b being identical to the MS1 with a low symmetry energy of 25 MeV and finally the APR EOS [129]. We constructed the $M - R$ graphs for all these cases, and we confronted the extracted data on masses and radii of the resulting static NSs with the three following constraints CSI, CSII and CSIII, also appearing in Fig. 1: the CSI constraint appeared first in Ref. [47] and indicates that the radius of an $1.4M_\odot$ mass NS must be $R_{1.4M_\odot} = 12.42^{+0.52}_{-0.99}$ while the radius of a $2M_\odot$ mass NS must be $R_{2M_\odot} = 12.11^{+1.11}_{-1.23}$ km. With regard to CSII, it appeared first in Ref. [56] and indicates that the radius of an $1.4M_\odot$ mass NS must be $R_{1.4M_\odot} = 12.33^{+0.76}_{-0.81}$ km. With regard to the CSIII constraint, it appeared first in Ref. [51] and indicates two things: first that the radius of a $1.6M_\odot$ mass NS has to be larger than $R_{1.6M_\odot} > 10.68^{+0.15}_{-0.04}$ km and, second, the radius of a NS corresponding to its maximum mass must satisfy $R_{M_{\max}} > 9.6^{+0.14}_{-0.03}$ km. The TOV equations are solved numerically in order to extract the Jordan frame masses and radii of the NSs and in order to construct the corresponding $M - R$ graphs. We used a Python-3-based numerical code which is based on the PYTOV-STT code [143]. We shall use the LSODA integration technique, and a double shooting method in order to find the optimal values of the initial conditions ν_c and φ_c defined in Eq. (27), which render the scalar field zero at numerical infinity. Let us further elaborate on the numerical integration technique. As we quoted above, the method we shall use is the LSODA, which is more powerful compared to the Runge-Kutta technique, due to the fact that the LSODA integration method is more appropriate for stiff differential equation problems. We solved separately the TOV equations for the interior and

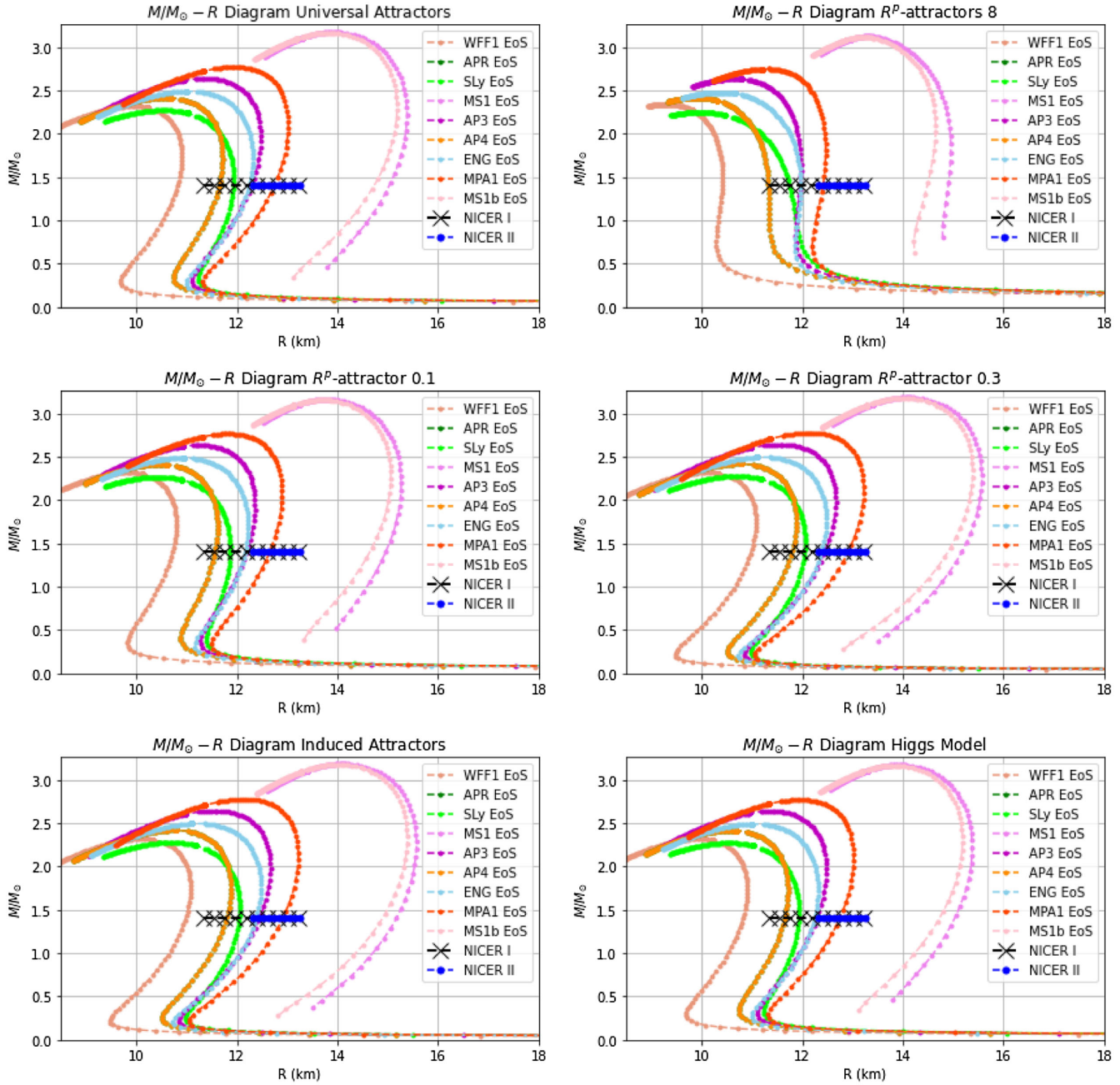

FIG. 2. The $M - R$ graphs for the universal attractors and the R^p attractors (three distinct model values), the induced inflation and Higgs inflation for the EOSs WFF1, SLy, APR, MS1, AP3, AP4, ENG, MPA1, MS1b versus the NICER I [131] and NICER II [58] constraints.

the exterior of the star, using approximately 160 values of the central density, and nearly 20000 grid points. The method is quite reliable because we used a double shooting technique to determine the accurate values for the ν_c and φ_c defined in Eq. (27), and specifically we optimized their values according to the rule that, for the optimal values, the scalar field vanishes at numerical infinity. The numerical infinity is actually determined by exactly this rule.

For all the $M - R$ graphs we shall plot, we included the NICER I constraint for $M = 1.4M_\odot$ NSs which is 90% credible [131] and constrains the radius of an $M = 1.4M_\odot$ to be $R_{1.4M_\odot} = 11.34$–13.23 km. Also recently, a more refined extension of the NICER constraint was introduced in [58] by taking into account the heavy black-widow binary pulsar PSR J0952-0607 with mass $M = 2.35 \pm 0.17$ [15]. The black widow pulsar PSR J0952-0607 is the heavier known NSs and we need to note that the NICER II constraint takes this into account. The results of our analysis are quite interesting, aligned with the NICER II constraints and indicate that these are satisfied only for

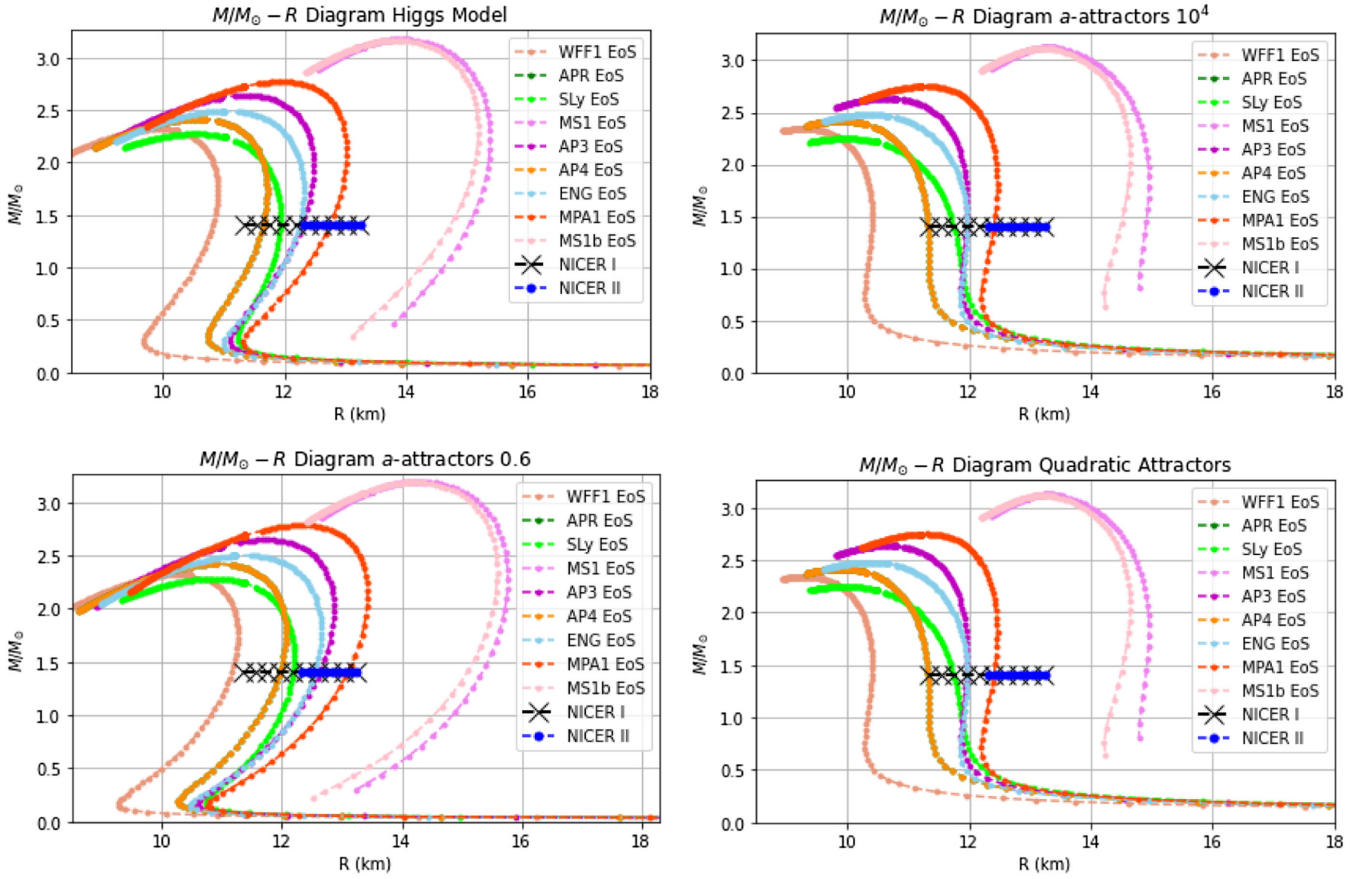

FIG. 3. The $M - R$ graphs for the universal attractors and the R^p attractors (three distinct model values), the induced inflation and Higgs inflation for the EOSs WFF1, SLy, APR, MS1, AP3, AP4, ENG, MPA1, MS1b versus the NICER I [131] and NICER II [58] constraints.

EOSs which yield the maximum masses of NSs inside the mass-gap region, but still lower that the causal three solar masses limit. The NICER II constrains the radius of a $M = 1.4M_\odot$ to be $R_{1.4M_\odot} = 12.33$–13.25 km. We shall refer to this new constraint as NICER II for simplicity hereafter. Also in the following Table VIII we present the two NICER I and NICER II constraints for reading convenience. The $M - R$ graphs of our analysis are presented in Figs. 2–5. In Fig. 2 we present the $M - R$ graphs for the universal attractors and the R^p attractors (three distinct model values), the induced inflation and Higgs inflation for the EOSs WFF1, SLy, APR, MS1, AP3, AP4, ENG, MPA1, MS1b versus the NICER I [131] and NICER II [58] constraints. In Fig. 3 we present the $M - R$ graphs for the universal attractors and the R^p attractors (three distinct model values), the induced inflation and Higgs inflation for the EOSs WFF1, SLy, APR, MS1, AP3, AP4, ENG, MPA1, MS1b versus the NICER I and NICER II constraints. In Fig. 4 we present the $M - R$ graphs for the universal attractors, the R^p attractors (three distinct model values), the induced inflation, the quadratic inflation, the Higgs inflation and the a attractors (two distinct model values) for the EOSs WFF1, SLy, APR, MS1 versus the NICER I and NICER II constraints, and finally in Fig. 5, the $M - R$ graphs are presented for all the aforementioned attractor models, for the EOSs AP3, AP4, ENG, MPA1, MS1b, confronted again with the NICER I, II constraints. Also in Table I we present the EOSs and the inflationary attractor models which yield a maximum NS mass inside the mass-gap region. In Tables II and III we present the confrontation of the radii of the NSs with the constraint CSI regarding $M \sim 2M_\odot$ NSs. In Tables IV and V we present the confrontation of the radii of the NSs with the constraint CSI regarding $M \sim 1.4M_\odot$ NSs. In Tables VI and VII we present the confrontation of the radii of the NSs with the constraint CSII regarding $M \sim 1.4M_\odot$ NSs. In Tables IX and X we present the confrontation of the radii of the NSs with the constraint CSIII regarding $M \sim 1.6M_\odot$ NSs, while in Tables XI and XII we present the confrontation of the radii of the NSs with the constraint CSIII regarding maximum mass NSs.

Now let us analyze the extracted data, and the results are deemed quite interesting. The most important result is that all the inflationary models are compatible with the NICER I and NICER II, and all the CSI, CSII, CSIII constraints, for the MPA1 EOS. More importantly, for

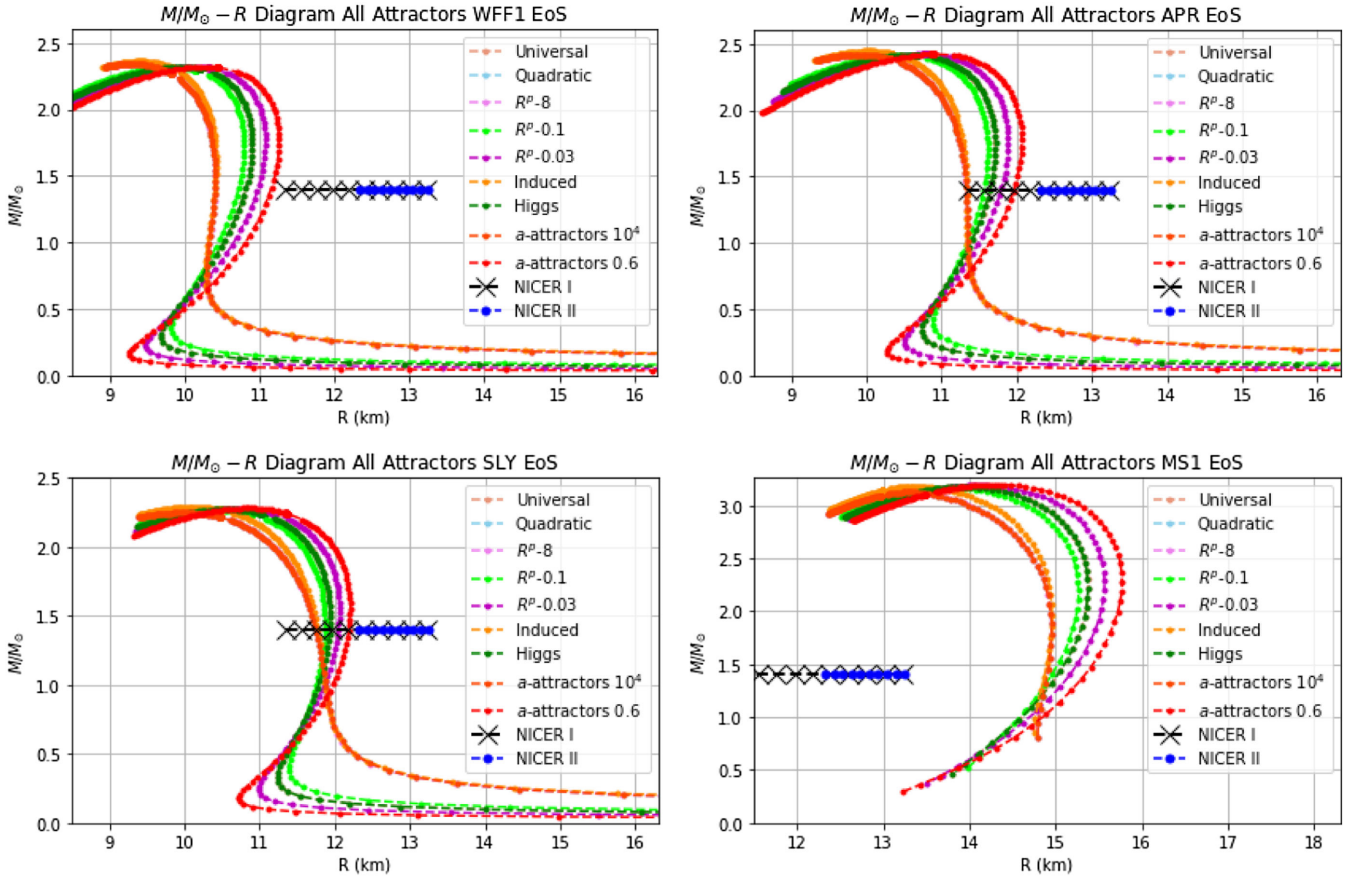

FIG. 4. The $M-R$ graphs for the universal attractors, the R^p attractors (three distinct model values), the induced inflation, the quadratic inflation, the Higgs inflation and the a attractors (two distinct model values) for the EOSs WFF1, SLy, APR, MS1 versus the NICER I [131] and NICER II [58] constraints.

this particular EOS, the maximum predicted NS masses are inside the mass gap region 2.5–5$M_\odot$, but well below the causal three solar masses limit of GR, which is respected. Recall that the causal EOS limit is very important so let us briefly recall what the causal EOS limit is, and why our result is aligned with this extreme GR limit, which also holds true in modified gravity theories [38]. The causality constraint is an important constraint for most reliable EOSs, which must be respected in order for an EOS to be considered reliable, In principle, when $dP/d\rho > 1$ in natural units, the EOS can be rendered superluminal, while when $P > \rho$, the EOSs can become ultrabaric. A related question of course is whether a superluminality predicting an EOS in terms of its sound speed can be incompatible with Lorentz invariance and of course causality. The answer to this question is no, nevertheless, the EOSs which become superluminal, do become superluminal for NSs energy densities for which the NSs are rendered hydrodynamically unstable [16], and this applies for stiff EOSs too. If we take into consideration the nuclear matter stability condition at high densities $\frac{dP}{d\rho} > 0$, in conjunction with the subluminality condition $\frac{dP}{d\rho} \leq 1$ (in natural units), a very well established GR originating limit for the maximum mass of static NSs is the so-called causal maximum mass limit [144,145],

$$M_{\max}^{\mathrm{CL}} = 3M_\odot \sqrt{\frac{5\times 10^{14}\ \mathrm{g/cm^3}}{\rho_u}}, \tag{128}$$

with ρ_u being the maximum density up to which the EOS is well known and the corresponding pressure is $P_u(\rho_u)$. The causal limit EOS is the following:

$$P_{sn}(\rho) = P_u(\rho_u) + (\rho - \rho_u)c^2. \tag{129}$$

Another well-known bound in astrophysics, also supporting the causal maximum mass limit, is the bound based on the maximum baryon mass of a static NS (all NSs with periods $P \gtrsim 3$ ms),

$$M_{\max} \leq 3M_\odot. \tag{130}$$

The causal maximum mass of a NS when rotation is taken into account is

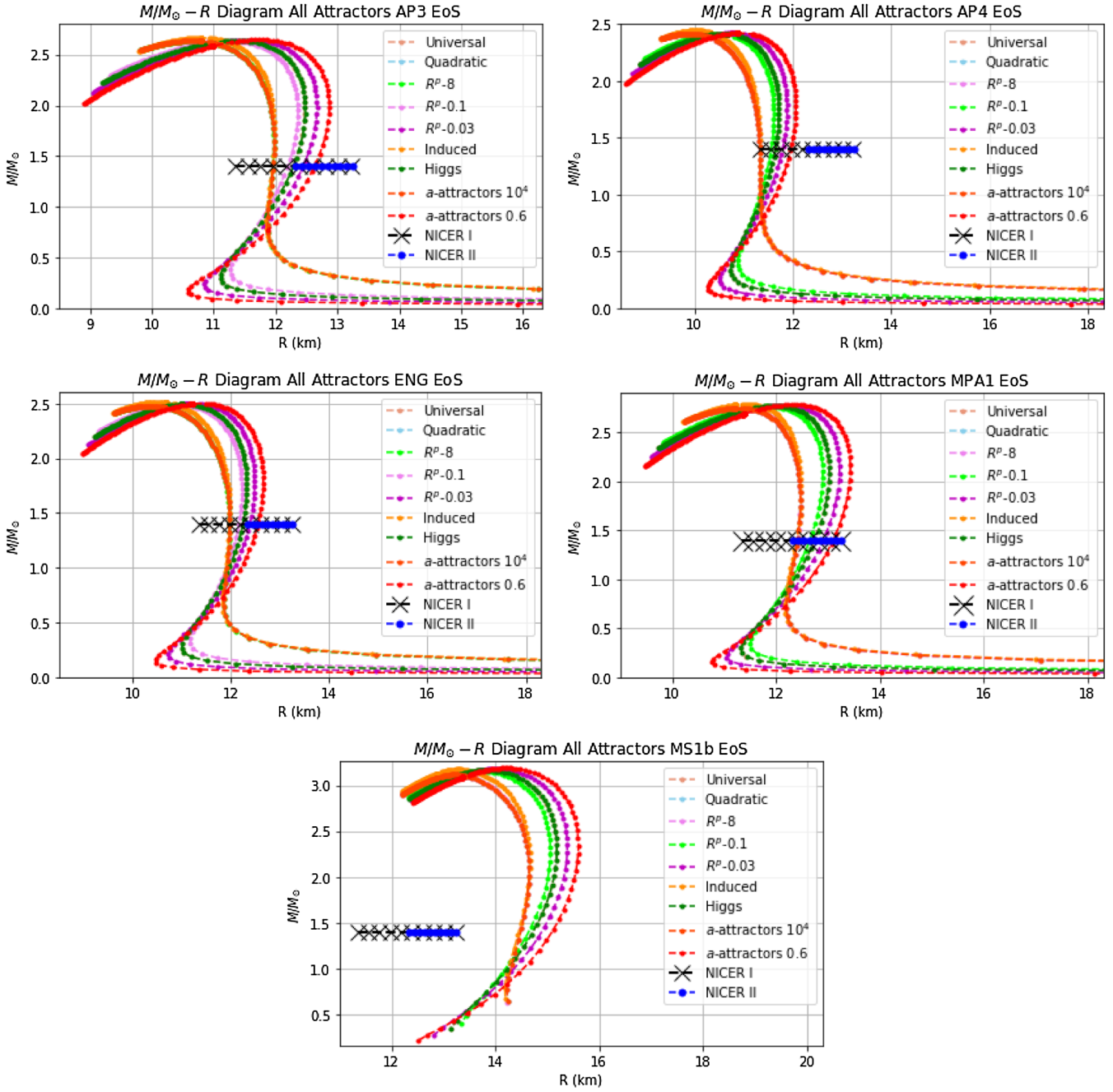

FIG. 5. The $M-R$ graphs for the universal attractors, the R^p attractors (three distinct model values), the induced inflation, the quadratic inflation, the Higgs inflation and the a attractors (two distinct model values) for the EOSs AP3, AP4, ENG, MPA1, MS1b versus the NICER I [131] and NICER II [58] constraints.

$$M_{\max}^{\mathrm{CL,rot}} = 3.89 M_\odot \sqrt{\frac{5\times 10^{14}\ \mathrm{g/cm^3}}{\rho_u}}. \qquad (131)$$

In our case it is remarkable that the MPA1 EOS produces results compatible with all the constraints for all the inflationary attractors and it is also compatible with the causal limit of maximum mass (128). The only EOSs which produce maximum masses beyond the causal limit of maximum mass (128) are the MS1 and MS1b, and remarkably, neither of the two produces $M-R$ graphs which are compatible with the constraints. In fact, neither of the two is compatible with even a single constraint. Another important feature of our analysis is the fact that if the NICER II constraints are taken into account, which recall that generated based on the heavier PSR J0952-0607, it seems that compatibility with the data comes hand in hand with models and EOSs which predict

TABLE I. Maximum masses for inflationary attractor NSs in the mass gap region.

Model	MPA1 EOS	MS1b EOS	AP3 EOS	ENG EOS	MS1 EOS
Universal attractors $M_{\rm MAX}$	$M_{\rm MPA1}=2.771M_\odot$	$M_{\rm MS1b}=3.167M_\odot$	$M_{\rm AP3}=2.638M_\odot$	$M_{\rm ENG}=x$	$M_{\rm MS1}=3.174M_\odot$
R^p-8 attractors $M_{\rm MAX}$	$M_{\rm MPA1}=2.749M_\odot$	$M_{\rm MS1b}=3.118M_\odot$	$M_{\rm AP3}=2.6359M_\odot$	$M_{\rm ENG}=x$	$M_{\rm MS1}=3.126M_\odot$
R^p-10^{-1} attractors $M_{\rm MAX}$	$M_{\rm MPA1}=2.765M_\odot$	$M_{\rm MS1b}=3.158M_\odot$	$M_{\rm AP3}=2.6357M_\odot$	$M_{\rm ENG}=x$	$M_{\rm MS1}=3.166M_\odot$
R^p-10^{-3} attractors $M_{\rm MAX}$	$M_{\rm MPA1}=2.778M_\odot$	$M_{\rm MS1b}=3.179M_\odot$	$M_{\rm AP3}=2.643M_\odot$	$M_{\rm ENG}=x$	$M_{\rm MS1}=3.186M_\odot$
Induced attractors $M_{\rm MAX}$	$M_{\rm MPA1}=2.788M_\odot$	$M_{\rm MS1b}=3.174M_\odot$	$M_{\rm AP3}=2.659M_\odot$	$M_{\rm ENG}=2.51M_\odot$	$M_{\rm MS1}=3.182M_\odot$
Higgs model $M_{\rm MAX}$	$M_{\rm MPA1}=2.771M_\odot$	$M_{\rm MS1b}=3.167M_\odot$	$M_{\rm AP3}=2.638M_\odot$	$M_{\rm ENG}=x$	$M_{\rm MS1}=3.175M_\odot$
α-10^4 attractors $M_{\rm MAX}$	$M_{\rm MPA1}=2.749M_\odot$	$M_{\rm MS1b}=3.117M_\odot$	$M_{\rm AP3}=2.636M_\odot$	$M_{\rm ENG}=x$	$M_{\rm MS1}=3.126M_\odot$
α-0.6 attractors $M_{\rm MAX}$	$M_{\rm MPA1}=2.784M_\odot$	$M_{\rm MS1b}=3.189M_\odot$	$M_{\rm AP3}=2.647M_\odot$	$M_{\rm ENG}=2.500M_\odot$	$M_{\rm MS1}=3.197M_\odot$
Quadratic attractors $M_{\rm MAX}$	$M_{\rm MPA1}=2.749M_\odot$	$M_{\rm MS1b}=3.117M_\odot$	$M_{\rm AP3}=2.636M_\odot$	$M_{\rm ENG}=x$	$M_{\rm MS1}=3.126M_\odot$

TABLE II. Inflationary attractors vs CSI for NS masses $M\sim 2M_\odot$, $R_{2M_\odot}=12.11^{+1.11}_{-1.23}$ km, for the SLy, APR, WFF1, MS1 and AP3 EOSs.

Model	SLy EOS	APR EOS	WFF1 EOS	MS1 EOS	AP3 EOS
Universal attractors radii	$R_{\rm SLy}=11.64$ km	$R_{\rm APR}=11.63$ km	$R_{\rm WFF1}=x$	$R_{\rm MS1}=x$	$R_{\rm AP3}=12.46$ km
R^p-8 attractors radii	$R_{\rm SLy}=11.15$ km	$R_{\rm APR}=11.08$ km	$R_{\rm WFF1}=x$	$R_{\rm MS1}=x$	$R_{\rm AP3}=11.89$ km
R^p-10^{-1} attractors radii	$R_{\rm SLy}=11.54$ km	$R_{\rm APR}=11.52$ km	$R_{\rm WFF1}=x$	$R_{\rm MS1}=x$	$R_{\rm AP3}=12.35$ km
R^p-10^{-3} attractors radii	$R_{\rm SLy}=11.78$ km	$R_{\rm APR}=11.785$ km	$R_{\rm WFF1}=11.01$ km	$R_{\rm MS1}=x$	$R_{\rm AP3}=12.66$ km
Induced attractors radii	$R_{\rm SLy}=11.17$ km	$R_{\rm APR}=11.08$ km	$R_{\rm WFF1}=x$	$R_{\rm MS1}=x$	$R_{\rm AP3}=11.94$ km
Higgs model radii	$R_{\rm SLy}=11.64$ km	$R_{\rm APR}=11.60$ km	$R_{\rm WFF1}=x$	$R_{\rm MS1}=x$	$R_{\rm AP3}=12.47$ km
α-10^4 attractors radii	$R_{\rm SLy}=11.17$ km	$R_{\rm APR}=11.00$ km	$R_{\rm WFF1}=x$	$R_{\rm MS1}=x$	$R_{\rm AP3}=11.86$ km
α-10^{-1} attractors radii	$R_{\rm SLy}=11.96$ km	$R_{\rm APR}=11.96$ km	$R_{\rm WFF1}=11.16$ km	$R_{\rm MS1}=x$	$R_{\rm AP3}=12.85$ km
Quadratic attractors radii	$R_{\rm SLy}=11.17$ km	$R_{\rm APR}=11.06$ km	$R_{\rm WFF1}=x$	$R_{\rm MS1}=x$	$R_{\rm AP3}=11.89$ km

TABLE III. Inflationary attractors vs CSI for NS masses $M\sim 2M_\odot$, $R_{2M_\odot}=12.11^{+1.11}_{-1.23}$ km, for the AP4, ENG, MPA1 and MS1b.

Model	AP4 EOS	ENG EOS	MPA1 EOS	MS1b EOS
Universal attractors radii	$R_{\rm AP4}=11.60$ km	$R_{\rm ENG}=12.22$ km	$R_{\rm MPA1}=13.01$ km	$R_{\rm MS1b}=x$
R^p-8 attractors radii	$R_{\rm AP4}=11.05$ km	$R_{\rm ENG}=11.74$ km	$R_{\rm MPA1}=112.44$ km	$R_{\rm MS1b}=x$
R^p-10^{-1} attractors radii	$R_{\rm AP4}=11.52$ km	$R_{\rm ENG}=12.14$ km	$R_{\rm MPA1}=12.89$ km	$R_{\rm MS1b}=x$
R^p-10^{-3} attractors radii	$R_{\rm AP4}=11.82$ km	$R_{\rm ENG}=12.42$ km	$R_{\rm MPA1}=13.21$ km	$R_{\rm MS1b}=x$
Induced attractors radii	$R_{\rm AP4}=11.15$ km	$R_{\rm ENG}=11.82$ km	$R_{\rm MPA1}=12.46$ km	$R_{\rm MS1b}=x$
Higgs model radii	$R_{\rm AP4}=11.63$ km	$R_{\rm ENG}=12.24$ km	$R_{\rm MPA1}=13.02$ km	$R_{\rm MS1b}=x$
α-10^4 attractors radii	$R_{\rm AP4}=11.08$ km	$R_{\rm ENG}=11.74$ km	$R_{\rm MPA1}=12.44$ km	$R_{\rm MS1b}=x$
α-10^{-1} attractors radii	$R_{\rm AP4}=12.01$ km	$R_{\rm ENG}=12.61$ km	$R_{\rm MPA1}=13.42$ km	$R_{\rm MS1b}=x$
Quadratic attractors radii	$R_{\rm AP4}=11.08$ km	$R_{\rm ENG}=11.68$ km	$R_{\rm MPA1}=12.44$ km	$R_{\rm MS1b}=x$

TABLE IV. Inflationary attractors vs CSI for NS masses $M\sim 1.4M_\odot$, $R_{1.4M_\odot}=12.42^{+0.52}_{-0.99}$, for the SLy, APR, WFF1, MS1 and AP3 EOSs.

Model	SLy EOS	APR EOS	WFF1 EOS	MS1 EOS	AP3 EOS
Universal attractors radii	$R_{\rm SLy}=11.93$ km	$R_{\rm APR}=11.64$ km	$R_{\rm WFF1}=x$	$R_{\rm MS1}=x$	$R_{\rm AP3}=x$
R^p-8 attractors radii	$R_{\rm SLy}=11.73$ km	$R_{\rm APR}=x$	$R_{\rm WFF1}=x$	$R_{\rm MS1}=x$	$R_{\rm AP3}=x$
R^p-10^{-1} attractors radii	$R_{\rm SLy}=11.85$ km	$R_{\rm APR}=11.55$ km	$R_{\rm WFF1}=x$	$R_{\rm MS1}=x$	$R_{\rm AP3}=12.18$ km
R^p-10^{-3} attractors radii	$R_{\rm SLy}=12.04$ km	$R_{\rm APR}=11.80$ km	$R_{\rm WFF1}=x$	$R_{\rm MS1}=x$	$R_{\rm AP3}=12.43$ km
Induced attractors radii	$R_{\rm SLy}=11.77$ km	$R_{\rm APR}=x$	$R_{\rm WFF1}=x$	$R_{\rm MS1}=x$	$R_{\rm AP3}=11.96$ km
Higgs model radii	$R_{\rm SLy}=11.93$ km	$R_{\rm APR}=11.64$ km	$R_{\rm WFF1}=x$	$R_{\rm MS1}=x$	$R_{\rm AP3}=12.28$ km
α-10^4 attractors radii	$R_{\rm SLy}=11.73$ km	$R_{\rm APR}=x$	$R_{\rm WFF1}=x$	$R_{\rm MS1}=x$	$R_{\rm AP3}=11.96$ km
α-10^{-1} attractors radii	$R_{\rm SLy}=12.18$ km	$R_{\rm APR}=11.95$ km	$R_{\rm WFF1}=x$	$R_{\rm MS1}=x$	$R_{\rm AP3}=12.65$ km
Quadratic attractors radii	$R_{\rm SLy}=11.75$ km	$R_{\rm APR}=11.64$ km	$R_{\rm WFF1}=x$	$R_{\rm MS1}=x$	$R_{\rm AP3}=11.96$ km

TABLE V. Inflationary attractors vs CSI for NS masses $M \sim 1.4M_{\odot}$, $R_{1.4M_{\odot}} = 12.42^{+0.52}_{-0.99}$, for the AP4, ENG, MPA1 and MS1b.

Model	AP4 EOS	ENG EOS	MPA1 EOS	MS1b EOS
Universal attractors radii	$R_{\rm AP4} = 11.64$ km	$R_{\rm ENG} = 12.23$ km	$R_{\rm MPA1} = 12.74$ km	$R_{\rm MS1b} = x$
R^p-8 attractors radii	$R_{\rm AP4} = 11.93$ km	$R_{\rm ENG} = x$	$R_{\rm MPA1} = 12.41$ km	$R_{\rm MS1b} = x$
R^p-10^{-1} attractors radii	$R_{\rm AP4} = 11.55$ km	$R_{\rm ENG} = 12.16$ km	$R_{\rm MPA1} = 12.64$ km	$R_{\rm MS1b} = x$
R^p-10^{-3} attractors radii	$R_{\rm AP4} = 11.80$ km	$R_{\rm ENG} = 12.38$ km	$R_{\rm MPA1} = x$	$R_{\rm MS1b} = x$
Induced attractors radii	$R_{\rm AP4} = x$	$R_{\rm ENG} = 11.97$ km	$R_{\rm MPA1} = 12.38$ km	$R_{\rm MS1b} = x$
Higgs model radii	$R_{\rm AP4} = 11.64$ km	$R_{\rm ENG} = 12.23$ km	$R_{\rm MPA1} = 12.74$ km	$R_{\rm MS1b} = x$
α-10^4 attractors radii	$R_{\rm AP4} = x$	$R_{\rm ENG} = 11.97$ km	$R_{\rm MPA1} = 12.41$ km	$R_{\rm MS1b} = x$
α-10^{-1} attractors radii	$R_{\rm AP4} = 11.95$ km	$R_{\rm ENG} = 12.55$ km	$R_{\rm MPA1} = x$	$R_{\rm MS1b} = x$
Quadratic attractors radii	$R_{\rm AP4} = 11.93$ km	$R_{\rm ENG} = 11.97$ km	$R_{\rm MPA1} = 12.41x$	$R_{\rm MS1b} = x$

TABLE VI. Inflationary attractors radii vs CSII for NS masses $M \sim 1.4M_{\odot}$, $R_{1.4M_{\odot}} = 12.33^{+0.76}_{-0.81}$ km, for the SLy, APR, WFF1, MS1 and AP3 EOSs.

Model	SLy EOS	APR EOS	WFF1 EOS	MS1 EOS	AP3 EOS
Universal attractors radii	$R_{\rm SLy} = 11.93$ km	$R_{\rm APR} = 11.64$ km	$R_{\rm WFF1} = x$	$R_{\rm MS1} = x$	$R_{\rm AP3} = 11.36$ km
R^p-8 attractors radii	$R_{\rm SLy} = 11.73$ km	$R_{\rm APR} = x$	$R_{\rm WFF1} = x$	$R_{\rm MS1} = x$	$R_{\rm AP3} = x$
R^p-10^{-1} attractors radii	$R_{\rm SLy} = 11.85$ km	$R_{\rm APR} = 11.55$ km	$R_{\rm WFF1} = x$	$R_{\rm MS1} = x$	$R_{\rm AP3} = 12.18$ km
R^p-10^{-3} attractors radii	$R_{\rm SLy} = 12.04$ km	$R_{\rm APR} = 11.80$ km	$R_{\rm WFF1} = x$	$R_{\rm MS1} = x$	$R_{\rm AP3} = 12.43$ km
Induced attractors radii	$R_{\rm SLy} = 11.77$ km	$R_{\rm APR} = x$	$R_{\rm WFF1} = x$	$R_{\rm MS1} = x$	$R_{\rm AP3} = 11.96$ km
Higgs model radii	$R_{\rm SLy} = 11.93$ km	$R_{\rm APR} = 11.64$ km	$R_{\rm WFF1} = x$	$R_{\rm MS1} = x$	$R_{\rm AP3} = 12.28$ km
α-10^4 attractors radii	$R_{\rm SLy} = 11.73$ km	$R_{\rm APR} = x$	$R_{\rm WFF1} = x$	$R_{\rm MS1} = x$	$R_{\rm AP3} = 11.96$ km
α-10^{-1} attractors radii	$R_{\rm SLy} = 12.18$ km	$R_{\rm APR} = 11.95$ km	$R_{\rm WFF1} = x$	$R_{\rm MS1} = x$	$R_{\rm AP3} = 12.65$ km
Quadratic attractors radii	$R_{\rm SLy} = 11.75$ km	$R_{\rm APR} = 11.64$ km	$R_{\rm WFF1} = x$	$R_{\rm MS1} = x$	$R_{\rm AP3} = 11.96$ km

TABLE VII. Inflationary attractors vs CSII for NS masses $M \sim 1.4M_{\odot}$, $R_{1.4M_{\odot}} = 12.33^{+0.76}_{-0.81}$ km, for the AP4, ENG, MPA1 and MS1b.

Model	AP4 EOS	ENG EOS	MPA1 EOS	MS1b EOS
Universal attractors radii	$R_{\rm AP4} = 11.64$ km	$R_{\rm ENG} = 12.23$ km	$R_{\rm MPA1} = 12.74$ km	$R_{\rm MS1b} = x$
R^p-8 attractors radii	$R_{\rm AP4} = 11.93$ km	$R_{\rm ENG} = x$	$R_{\rm MPA1} = 12.41$ km	$R_{\rm MS1b} = x$
R^p-10^{-1} attractors radii	$R_{\rm AP4} = 11.55$ km	$R_{\rm ENG} = 12.16$ km	$R_{\rm MPA1} = 12.64$ km	$R_{\rm MS1b} = x$
R^p-10^{-3} attractors radii	$R_{\rm AP4} = 11.80$ km	$R_{\rm ENG} = 12.38$ km	$R_{\rm MPA1} = x$	$R_{\rm MS1b} = x$
Induced attractors radii	$R_{\rm AP4} = x$	$R_{\rm ENG} = 11.97$ km	$R_{\rm MPA1} = 12.38$ km	$R_{\rm MS1b} = x$
Higgs model radii	$R_{\rm AP4} = 11.64$ km	$R_{\rm ENG} = 12.23$ km	$R_{\rm MPA1} = 12.74$ km	$R_{\rm MS1b} = x$
α-10^4 attractors radii	$R_{\rm AP4} = x$	$R_{\rm ENG} = 11.97$ km	$R_{\rm MPA1} = 12.41$ km	$R_{\rm MS1b} = x$
α-10^{-1} attractors radii	$R_{\rm AP4} = 11.95$ km	$R_{\rm ENG} = 12.55$ km	$R_{\rm MPA1} = x$	$R_{\rm MS1b} = x$
Quadratic attractors radii	$R_{\rm AP4} = 11.93$ km	$R_{\rm ENG} = 11.97$ km	$R_{\rm MPA1} = 12.41x$	$R_{\rm MS1b} = x$

maximum masses beyond 2.5 solar masses, thus in the mass gap region and at the same time below the three solar masses causal limit. This for example becomes true for all the inflationary models studied, only for the MPA1 EOS, so the question is, is this EOS so important? Is it possible that this EOS describes NSs at a fundamental level? The future observations will show, but for the moment we report this interesting behavior. Of course there are other EOSs that are compatible with the NICER II constraint, such as the ENG and AP3, which remarkably also predict maximum masses inside the mass gap region and below the three solar masses causal limit, but in these EOSs, only some inflationary attractors produce viable results, for example the Higgs, the a attractors and the R^p attractors, but in the case of the MPA1 EOS, all the inflationary models are compatible with the NICER II observations. Another major outcome of this work is that

TABLE VIII. NICER I AND NICER II constraints for the radius of a $M = 1.4M_{\odot}$ NS.

NICER I	11.34 km $< R_{1.4M_{\odot}} < 13.23$ km [131]
NICER II	12.33 km $< R_{1.4M_{\odot}} < 13.25$ km [58]

TABLE IX. Inflationary attractors vs CSIII for NS masses $M \sim 1.6M_{\odot}$, $R_{1.6M_{\odot}} > 10.68^{+0.15}_{-0.04}$ km, for the SLy, APR, WFF1, MS1 and AP3 EOSs.

Model	SLy EOS	APR EOS	WFF1EOS	MS1 EOS	AP3 EOS
Universal attractors radii	$R_{\rm SLy} = 11.92$ km	$R_{\rm APR} = 11.70$ km	$R_{\rm WFF1} = 11.68$ km	$R_{\rm MS1} = 13.99$ km	$R_{\rm AP3} = 12.41$ km
R^p-8 attractors radii	$R_{\rm SLy} = 11.89$ km	$R_{\rm APR} = 11.28$ km	$R_{\rm WFF1} = 10.40$ km	$R_{\rm MS1} = 14.93$ km	$R_{\rm AP3} = 11.97$ km
R^p-10^{-1} attractors radii	$R_{\rm SLy} = 11.85$ km	$R_{\rm APR} = 11.61$ km	$R_{\rm WFF1} = x$	$R_{\rm MS1} = 15.11$ km	$R_{\rm AP3} = 12.29$ km
R^p-10^{-3} attractors radii	$R_{\rm SLy} = 11.80$ km	$R_{\rm APR} = 11.59$ km	$R_{\rm WFF1} = x$	$R_{\rm MS1} = 15.20$ km	$R_{\rm AP3} = 12.34$ km
Induced attractors radii	$R_{\rm SLy} = 11.68$ km	$R_{\rm APR} = 11.32$ km	$R_{\rm WFF1} = x$	$R_{\rm MS1} = 14.92$ km	$R_{\rm AP3} = 11.97$ km
Higgs model radii	$R_{\rm SLy} = 11.92$ km	$R_{\rm APR} = 11.70$ km	$R_{\rm WFF1} = 10.89$ km	$R_{\rm MS1} = 14.92$ km	$R_{\rm AP3} = 11.93$ km
α-10^{4} attractors radii	$R_{\rm SLy} = 11.64$ km	$R_{\rm APR} = 11.29$ km	$R_{\rm WFF1} = x$	$R_{\rm MS1} = 14.94$ km	$R_{\rm AP3} = 11.97$ km
α-10^{-1} attractors radii	$R_{\rm SLy} = 12.20$ km	$R_{\rm APR} = 12.04$ km	$R_{\rm WFF1} = 11.23$ km	$R_{\rm MS1} = 15.49$ km	$R_{\rm AP3} = 12.76$ km
Quadratic attractors radii	$R_{\rm SLy} = 11.64$ km	$R_{\rm APR} = 11.29$ km	$R_{\rm WFF1} = x$	$R_{\rm MS1} = 14.94$ km	$R_{\rm AP3} = 11.97$ km

TABLE X. Inflationary attractors vs CSIII for NS masses $M \sim 1.6M_{\odot}$, $R_{1.6M_{\odot}} > 10.68^{+0.15}_{-0.04}$ km, for the AP4, ENG, MPA1 and MS1b.

Model	AP4 EOS	ENG EOS	MPA1 EOS	MS1b EOS
Universal attractors radii	$R_{\rm AP4} = 11.70$ km	$R_{\rm ENG} = 12.30$ km	$R_{\rm MPA1} = 12.87$ km	$R_{\rm MS1b} = 14.90$ km
R^p-8 attractors radii	$R_{\rm AP4} = 11.28$ km	$R_{\rm ENG} = 11.94$ km	$R_{\rm MPA1} = 12.45$ km	$R_{\rm MS1b} = 14.59$ km
R^p-10^{-1} attractors radii	$R_{\rm AP4} = 11.61$ km	$R_{\rm ENG} = 12.21$ km	$R_{\rm MPA1} = 12.79$ km	$R_{\rm MS1b} = 14.78$ km
R^p-10^{-3} attractors radii	$R_{\rm AP4} = 11.86$ km	$R_{\rm ENG} = 12.45$ km	$R_{\rm MPA1} = 12.15$ km	$R_{\rm MS1b} = 15.04$ km
Induced attractors radii	$R_{\rm AP4} = 11.32$ km	$R_{\rm ENG} = 11.96$ km	$R_{\rm MPA1} = 12.44$ km	$R_{\rm MS1b} = 14.49$ km
Higgs model radii	$R_{\rm AP4} = 11.70$ km	$R_{\rm ENG} = 12.30$ km	$R_{\rm MPA1} = 12.87$ km	$R_{\rm MS1b} = 14.90$ km
α-10^{4} attractors radii	$R_{\rm AP4} = 11.28$ km	$R_{\rm ENG} = 11.95$ km	$R_{\rm MPA1} = 12.44$ km	$R_{\rm MS1b} = 14.55$ km
α-10^{-1} attractors radii	$R_{\rm AP4} = 10.99$ km	$R_{\rm ENG} = 12.63$ km	$R_{\rm MPA1} = 13.22$ km	$R_{\rm MS1b} = 15.22$ km
Quadratic attractors radii	$R_{\rm AP4} = 11.28$ km	$R_{\rm ENG} = 11.95$ km	$R_{\rm MPA1} = 12.44$ km	$R_{\rm MS1b} = 14.55$ km

cosmologically indistinguishable inflationary attractors become distinguished in NSs. This feature, however, seems to be EOS and model dependent, since for example for the APR EOS, the quadratic attractors, the a attractors and the R^p-8 attractors produce overlapping results. Regarding the constraint CSI, the WFF1, the MS1 and MS1b EOS are excluded completely (apart for some cases of the a attractors and R^p attractors regarding

TABLE XI. Inflationary attractors maximum NS masses and the corresponding radii vs CSIII, $R_{M_{\rm max}} > 9.6^{+0.14}_{-0.03}$ km, for the SLy, APR, WFF1, MS1 and AP3 EOSs.

Model	APR EOS	SLy EOS	WFF1 EOS	MS1 EOS	AP3 EOS
Universal attractors $M_{\rm max}$	$M_{\rm APR} = 2.41M_{\odot}$	$M_{\rm SLy} = 2.27M_{\odot}$	$M_{\rm WFF1} = 2.32M_{\odot}$	$M_{\rm MS1} = 3.17M_{\odot}$	$M_{\rm AP3} = 2.63M_{\odot}$
Universal attractors radii	$R_{\rm APR} = 10.54$ km	$R_{\rm SLy} = 10.56$ km	$R_{\rm WFF1} = 9.91$ km	$R_{\rm MS1} = 13.93$ km	$R_{\rm AP3} = 11.35$ km
R^p-8 attractors $M_{\rm max}$	$M_{\rm APR} = 2.41M_{\odot}$	$M_{\rm SLy} = 2.24M_{\odot}$	$M_{\rm WFF1} = 2.34M_{\odot}$	$M_{\rm MS1} = 3.12M_{\odot}$	$M_{\rm AP3} = 2.63M_{\odot}$
R^p-8 attractors radii	$R_{\rm APR} = 9.91$ km	$R_{\rm SLy} = 9.96$ km	$R_{\rm WFF1} = 9.28$ km	$R_{\rm MS1} = 13.30$ km	$R_{\rm AP3} = 10.67$ km
R^p-10^{-1} attractors $M_{\rm max}$	$M_{\rm APR} = 2.41M_{\odot}$	$M_{\rm SLy} = 2.26M_{\odot}$	$M_{\rm WFF1} = 2.31M_{\odot}$	$M_{\rm MS1} = 3.16M_{\odot}$	$M_{\rm AP3} = 2.63M_{\odot}$
R^p-10^{-1} attractors radii	$R_{\rm APR} = 10.49$ km	$R_{\rm SLy} = 10.43$ km	$R_{\rm WFF1} = 9.83$ km	$R_{\rm MS1} = 13.81$ km	$R_{\rm AP3} = 11.24$ km
R^p-10^{-3} attractors $M_{\rm max}$	$M_{\rm APR} = 2.42M_{\odot}$	$M_{\rm SLy} = 2.27M_{\odot}$	$M_{\rm WFF1} = 2.32M_{\odot}$	$M_{\rm MS1} = 3.18M_{\odot}$	$M_{\rm AP3} = 2.64M_{\odot}$
R^p-10^{-3} attractors radii	$R_{\rm APR} = 10.77$ km	$R_{\rm SLy} = 10.72$ km	$R_{\rm WFF1} = 10.09$ km	$R_{\rm MS1} = 14.09$ km	$R_{\rm AP3} = 11.55$ km
Induced attractors $M_{\rm max}$	$M_{\rm APR} = 2.44M_{\odot}$	$M_{\rm SLy} = 2.28M_{\odot}$	$M_{\rm WFF1} = 2.36M_{\odot}$	$M_{\rm MS1} = 3.18M_{\odot}$	$M_{\rm AP3} = 2.66M_{\odot}$
Induced attractors radii	$R_{\rm APR} = 10.04$ km	$R_{\rm SLy} = 10.10$ km	$R_{\rm WFF1} = 9.42$ km	$R_{\rm MS1} = 13.36$ km	$R_{\rm AP3} = 10.80$ km
Higgs model $M_{\rm max}$	$M_{\rm APR} = 2.41M_{\odot}$	$M_{\rm SLy} = 2.27M_{\odot}$	$M_{\rm WFF1} = 2.32M_{\odot}$	$M_{\rm MS1} = 3.17M_{\odot}$	$M_{\rm AP3} = 2.63M_{\odot}$
Higgs model radii	$R_{\rm APR} = 10.57$ km	$R_{\rm SLy} = 10.56$ km	$R_{\rm WFF1} = 9.91$ km	$R_{\rm MS1} = 13.91$ km	$R_{\rm AP3} = 11.35$ km
α-10^{4} attractors $M_{\rm max}$	$M_{\rm APR} = 2.41M_{\odot}$	$M_{\rm SLy} = 2.24M_{\odot}$	$M_{\rm WFF1} = 2.34M_{\odot}$	$M_{\rm MS1} = 3.12M_{\odot}$	$M_{\rm AP3} = 2.63M_{\odot}$
α-10^{4} attractors radii	$R_{\rm APR} = 9.89$ km	$R_{\rm SLy} = 9.98$ km	$R_{\rm WFF1} = 9.29$ km	$R_{\rm MS1} = 13.31$ km	$R_{\rm AP3} = 10.65$ km
α-10^{-1} attractors $M_{\rm max}$	$M_{\rm APR} = 2.42M_{\odot}$	$M_{\rm SLy} = 2.28M_{\odot}$	$M_{\rm WFF1} = 2.32M_{\odot}$	$M_{\rm MS1} = 3.19M_{\odot}$	$M_{\rm AP3} = 2.64M_{\odot}$
α-10^{-1} attractors radii	$R_{\rm APR} = 10.89$ km	$R_{\rm SLy} = 10.81$ km	$R_{\rm WFF1} = 10.22$ km	$R_{\rm MS1} = 14.29$ km	$R_{\rm AP3} = 11.72$ km
Quadratic attractors $M_{\rm max}$	$M_{\rm APR} = 2.41M_{\odot}$	$M_{\rm SLy} = 2.24M_{\odot}$	$M_{\rm WFF1} = 2.34M_{\odot}$	$M_{\rm MS1} = 3.12M_{\odot}$	$M_{\rm AP3} = 2.63M_{\odot}$
Quadratic attractors radii	$R_{\rm APR} = 9.89$ km	$R_{\rm SLy} = 9.96$ km	$R_{\rm WFF1} = 9.28$ km	$R_{\rm MS1} = 13.31$ km	$R_{\rm AP3} = 10.67$ km

TABLE XII. Inflationary attractors maximum NS masses and the correspondent vs CSIII, $R_{M_{\max}} > 9.6^{+0.14}_{-0.03}$ km, for the AP4, ENG, MPA1 and MS1b.

Model	AP4 EOS	ENG EOS	MPA1 EOS	MS1b EOS
Universal attractors $M_{\max}$	$M_{\rm AP4} = 2.41M_\odot$	$M_{\rm ENG} = 2.49M_\odot$	$M_{\rm MPA1} = 2.77M_\odot$	$M_{\rm MS1b} = 3.16M_\odot$
Universal attractors radii	$R_{\rm AP4} = 10.54$ km	$R_{\rm ENG} = 11.00$ km	$R_{\rm MPA1} = 11.94$ km	$R_{\rm MS1b} = 13.83$ km
R^p-8 attractors $M_{\max}$	$M_{\rm AP4} = 2.41M_\odot$	$M_{\rm ENG} = 2.47M_\odot$	$M_{\rm MPA1} = 2.74M_\odot$	$M_{\rm MS1b} = 3.11M_\odot$
R^p-8 attractors radii	$R_{\rm AP4} = 9.91$ km	$R_{\rm ENG} = 10.36$ km	$R_{\rm MPA1} = 11.33$ km	$R_{\rm MS1b} = 13.21$ km
R^p-10^{-1} attractors $M_{\max}$	$M_{\rm AP4} = 2.41M_\odot$	$M_{\rm ENG} = 2.48M_\odot$	$M_{\rm MPA1} = 2.76M_\odot$	$M_{\rm MS1b} = 3.15M_\odot$
R^p-10^{-1} attractors radii	$R_{\rm AP4} = 10.49$ km	$R_{\rm ENG} = 10.92$ km	$R_{\rm MPA1} = 11.82$ km	$R_{\rm MS1b} = 13.73$ km
R^p-10^{-3} attractors $M_{\max}$	$M_{\rm AP4} = 2.42M_\odot$	$M_{\rm ENG} = 2.49M_\odot$	$M_{\rm MPA1} = 2.77M_\odot$	$M_{\rm MS1b} = 3.17M_\odot$
R^p-10^{-3} attractors radii	$R_{\rm AP4} = 10.77$ km	$R_{\rm ENG} = 11.11$ km	$R_{\rm MPA1} = 12.15$ km	$R_{\rm MS1b} = 14.06$ km
Induced attractors $M_{\max}$	$M_{\rm AP4} = 2.44M_\odot$	$M_{\rm ENG} = 2.51M_\odot$	$M_{\rm MPA1} = 2.78M_\odot$	$M_{\rm MS1b} = 3.17M_\odot$
Induced attractors radii	$R_{\rm AP4} = 10.04$ km	$R_{\rm ENG} = 10.49$ km	$R_{\rm MPA1} = 11.41$ km	$R_{\rm MS1b} = 13.29$ km
Higgs model $M_{\max}$	$M_{\rm AP4} = 2.41M_\odot$	$M_{\rm ENG} = 2.49M_\odot$	$M_{\rm MPA1} = 2.77M_\odot$	$M_{\rm MS1b} = 3.16M_\odot$
Higgs model radii	$R_{\rm AP4} = 10.57$ km	$R_{\rm ENG} = 11.01$ km	$R_{\rm MPA1} = 11.94$ km	$R_{\rm MS1b} = 13.83$ km
α-10^4 attractors $M_{\max}$	$M_{\rm AP4} = 2.41M_\odot$	$M_{\rm ENG} = 2.47M_\odot$	$M_{\rm MPA1} = 2.342M_\odot$	$M_{\rm MS1b} = 2.417M_\odot$
α-10^4 attractors radii	$R_{\rm AP4} = 9.89$ km	$R_{\rm ENG} = 10.36$ km	$R_{\rm MPA1} = 12.44$ km	$R_{\rm MS1b} = 14.55$ km
α-10^{-1} attractors $M_{\max}$	$M_{\rm AP4} = 2.42M_\odot$	$M_{\rm ENG} = 2.50M_\odot$	$M_{\rm MPA1} = 2.78M_\odot$	$M_{\rm MS1b} = 3.18M_\odot$
α-10^{-1} attractors radii	$R_{\rm AP4} = 10.89$ km	$R_{\rm ENG} = 11.48$ km	$R_{\rm MPA1} = 12.33$ km	$R_{\rm MS1b} = 14.22$ km
Quadratic attractors $M_{\max}$	$M_{\rm AP4} = 2.41M_\odot$	$M_{\rm ENG} = 2.47M_\odot$	$M_{\rm MPA1} = 2.74M_\odot$	$M_{\rm MS1b} = 3.11M_\odot$
Quadratic attractors radii	$R_{\rm AP4} = 9.89$ km	$R_{\rm ENG} = 10.36$ km	$R_{\rm MPA1} = 11.32$ km	$R_{\rm MS1b} = 13.21$ km

the WFF1) and the same applies for the CSII constraint. Regarding the CSIII constraints, only the WFF1 EOS produces results which are in most cases of inflationary attractors, incompatible with CSIII. The full results of the incompatibility of certain inflationary attractor models and EOSs, with the observational data and the existing constraints, can be found in the presented tables. We highlighted the most significant outcomes of this work, and as it seems, the MPA1 EOS seems to play an important role, while the WFF1, MS1 and MS1b seem to be entirely out of the equation, regarding a viable description of static NSs.

Before closing, let us discuss an important issue related with the discrimination of inflationary attractors on NSs, the % difference between the NS masses for different models of attractors and the differences in NS masses corresponding to piecewise polytropic and polytropic EOSs. It is vital that the differences between the masses using piecewise polytropic EOSs and ordinary polytropic EOSs to be lower than the differences between NS masses corresponding to inflationary attractors. In Table XIII we present the maximum masses of all the inflationary attractors for the piecewise polytropic MPA1 EOS and for the ordinary polytropic MPA1 EOS. The difference in the maximum mass between the different attractors for the piecewise polytropic MPA1 EOS varies from the minimum value $\sim\mathcal{O}(0.8\%)$ to the maximum value $\sim\mathcal{O}(1.27\%)$, while the average differences between the piecewise polytropic and the ordinary polytropic MPA1 EOS is of the order $\sim\mathcal{O}(0.1\%)$. Thus this feature may somehow obscure the discrimination of different attractors in NSs and it is a reportable feature, because the differences in maximum masses may be within the limits of errors in determining the mass of the NS.

TABLE XIII. Comparison of the maximum masses for all the inflationary attractors NSs for the piecewise and ordinary polytropic MPA1 EOS.

Model	MPA1 piecewise polytropic EOS	MPA1 ordinary polytropic EOS
Universal attractors $M_{\rm MAX}$	$M^{pp}_{\rm MPA1} = 2.771M_\odot$	$M^{p}_{\rm MPA1} = 2.77433M_\odot$
R^p-8 attractors $M_{\rm MAX}$	$M^{pp}_{\rm MPA1} = 2.749M_\odot$	$M^{p}_{\rm MPA1} = 2.74571M_\odot$
R^p-10^{-1} attractors $M_{\rm MAX}$	$M^{pp}_{\rm MPA1} = 2.765M_\odot$	$M^{p}_{\rm MPA1} = 2.76804M_\odot$
R^p-10^{-3} attractors $M_{\rm MAX}$	$M^{pp}_{\rm MPA1} = 2.778M_\odot$	$M^{p}_{\rm MPA1} = 2.78078M_\odot$
Induced attractors $M_{\rm MAX}$	$M^{pp}_{\rm MPA1} = 2.788M_\odot$	$M^{p}_{\rm MPA1} = 2.79107M_\odot$
Higgs model $M_{\rm MAX}$	$M^{pp}_{\rm MPA1} = 2.771M_\odot$	$M^{p}_{\rm MPA1} = 2.7735M_\odot$
α-10^4 attractors $M_{\rm MAX}$	$M^{pp}_{\rm MPA1} = 2.749M_\odot$	$M^{p}_{\rm MPA1} = 2.74598M_\odot$
α-0.6 attractors $M_{\rm MAX}$	$M^{pp}_{\rm MPA1} = 2.784M_\odot$	$M^{p}_{\rm MPA1} = 2.78707M_\odot$
Quadratic attractors $M_{\rm MAX}$	$M^{pp}_{\rm MPA1} = 2.749M_\odot$	$M^{p}_{\rm MPA1} = 2.75175M_\odot$

III. CONCLUDING REMARKS

In this work we studied static NS phenomenology in the context of various inflationary attractors using a large sample of EOSs adopting the piecewise polytropic EOS approach. The inflationary attractors we considered have a high cosmological significance and specifically we considered the universal attractors, the R^p attractors (three distinct model values), the induced inflation, the quadratic inflation, the Higgs inflation and the a attractors (two distinct model values). Regarding the EOSs, we used the WFF1, the SLy, the APR, the MS1, the AP3, the AP4, the ENG, the MPA1 and the MS1b ones, each of which has its own phenomenological significance. After numerically solving the TOV equations, we extracted the Jordan frame masses M and the Jordan frame radii R for all the aforementioned models and EOSs and we constructed the corresponding $M-R$ diagrams. We also confronted the models and EOSs with the observational and theoretical constraints. We considered the NICER constraints and also a modified version of the NICER constraints, which we called NICER II, introduced in [58], which was constructed by taking into account the heavy black-widow binary pulsar PSR J0952-0607 with mass $M = 2.35 \pm 0.17$ [15]. The NICER II constraint, indicates that the radius of a $M = 1.4M_\odot$ must be $R_{1.4M_\odot} = 12.33$–13.25 km. We also considered several theoretical constraints which are also based on observations, which we called CSI, CSII and CSIII. The CSI was introduced in Ref. [47] and indicates that the radius of an $1.4M_\odot$ mass NS must be $R_{1.4M_\odot} = 12.42^{+0.52}_{-0.99}$ while the radius of an $2M_\odot$ mass NS must be $R_{2M_\odot} = 12.11^{+1.11}_{-1.23}$ km. The second constraint we considered we named it CSII and was introduced in Ref. [56] and indicates that the radius of an $1.4M_\odot$ mass NS must be $R_{1.4M_\odot} = 12.33^{+0.76}_{-0.81}$ km. Moreover, we considered a third constraint, namely CSIII, which was introduced in Ref. [51] and indicates that the radius of an $1.6M_\odot$ mass NS must be larger than $R_{1.6M_\odot} > 10.68^{+0.15}_{-0.04}$ km, while when the radius of a NS with maximum mass is considered, it must be larger than $R_{M_{\max}} > 9.6^{+0.14}_{-0.03}$ km.

Our results are deemed interesting and are listed below:

(i) In the context of our work, it is possible to discriminate inflationary attractors which at the cosmological level are indistinguishable using the $M-R$ graphs. This feature though is model dependent and also EOS dependent, since for some EOSs and some cosmological models, the $M-R$ graphs we produced are identical. This for example occurred for the APR EOS and for the quadratic attractors, the a attractors and the R^p-8 attractors. Also the differences may be within the errors of the experimental limits, thus the discrimination has limitations.

(ii) Among all the EOSs, the only EOS which is compatible with all the constraints, theoretical and observational, is the MPA1, for all the inflationary models considered in this work. It is remarkable that the maximum masses for this EOS are inside the mass-gap region, with $M > 2.5M_\odot$, but lower than the three solar masses causal limit.

(iii) As the NICER constraints are pushed towards larger radii, it seems that EOSs which produce maximum masses in the mass gap region, with $M > 2.5M_\odot$, but lower than the three solar masses causal limit, are favored and compatible with the modified NICER constraints.

(iv) The only EOSs which produce maximum masses beyond the causal limit of three solar masses [see Eq. (128)] are the MS1 and MS1b, and remarkably, neither of the two produces $M-R$ graphs which are compatible with the constraints. In fact, neither of the two is compatible with even a single constraint.

(v) Among all EOSs we considered, the MPA1 EOS seems to play an important role, while the WFF1, MS1 and MS1b seem to be entirely ruled out, regarding a viable description of static NSs.

An important feature to note is that, as the NICER constraints are pushed to higher radii, by taking into account the PSR J0952-0607, it seems that the compatibility with the theoretical and observational constraints comes hand in hand with models and EOSs which generated maximum radii beyond the mass-gap region with $M > 2.5M_\odot$ and below the three solar masses causal EOSs limit. In our case, this occurs in a flawless way for the MPA1 EOS, which is compatible with all the constraints. This feature of course can be met in several other distinguished cases, for example for the ENG and AP3 EOSs and for the Higgs, the a attractors and the R^p attractor models, but in the case of the MPA1 EOS we found that all the models we considered are compatible with all the theoretical and observational constraints we considered in this article. Thus the question is, does the MPA1 EOS play an important role in NS physics, or is this multicompatibility with the constraints of this specific EOS accidental? Is this EOS fundamental for the NSs nuclear matter? We cannot tell, however it is reportable to say the least. It is notable that in the literature there exist articles that also find nice compatibility properties of the MPA1 EOS with the data, see for example Ref. [146]. We anticipate future observations to see whether heavy NSs exist in nature, heavier that the current $2.35M_\odot$ solar masses limit corresponding to the PSR J0952-0607. If NSs are found well inside the mass-gap region, beyond the $2.5M_\odot$ limit, but to our opinion below the causal three solar masses limit, this will be sensational and

decisive on whether modifications of GR are needed or not. Nature will tell us whether GR is all that is needed for the description of astrophysical phenomena, or whether GR is a lower limit of some effective theory active in extreme gravity astrophysical and cosmological phenomena. For the moment GR suffices though.

ACKNOWLEDGMENTS

This work was supported by MINECO (Spain), Project No. PID2019–104397GB-I00 (S. D. O.). This work by S. D. O. was also partially supported by the program Unidad de Excelencia Maria de Maeztu CEX2020-001058-M, Spain.

[1] B. P. Abbott *et al.* (LIGO Scientific and Virgo Collaborations), Phys. Rev. Lett. **119**, 161101 (2017).
[2] R. Abbott *et al.* (LIGO Scientific and Virgo Collaborations), Astrophys. J. Lett. **896**, L44 (2020).
[3] J. M. Ezquiaga and M. Zumalacárregui, Phys. Rev. Lett. **119**, 251304 (2017).
[4] T. Baker, E. Bellini, P. G. Ferreira, M. Lagos, J. Noller, and I. Sawicki, Phys. Rev. Lett. **119**, 251301 (2017).
[5] P. Creminelli and F. Vernizzi, Phys. Rev. Lett. **119**, 251302 (2017).
[6] J. Sakstein and B. Jain, Phys. Rev. Lett. **119**, 251303 (2017).
[7] S. D. Odintsov, V. K. Oikonomou, and F. P. Fronimos, Nucl. Phys. **B958**, 115135 (2020).
[8] V. K. Oikonomou, Classical Quantum Gravity **38**, 195025 (2021).
[9] V. K. Oikonomou, P. D. Katzanis, and I. C. Papadimitriou, Classical Quantum Gravity **39**, 095008 (2022).
[10] S. Nojiri, S. D. Odintsov, and V. K. Oikonomou, Phys. Rep. **692**, 1 (2017).
[11] S. Capozziello and M. De Laurentis, Phys. Rep. **509**, 167 (2011);
[12] V. Faraoni and S. Capozziello, Fundam. Theor. Phys. **170** (2010).
[13] S. Nojiri and S. D. Odintsov, Phys. Rep. **505**, 59 (2011);
[14] R. Abbott *et al.* (LIGO Scientific and Virgo Collaborations), Astrophys. J. Lett. **896**, L44 (2020).
[15] R. W. Romani, D. Kandel, A. V. Filippenko, T. G. Brink, and W. Zheng, Astrophys. J. Lett. **934**, L18 (2022).
[16] P. Haensel, A. Y. Potekhin, and D. G. Yakovlev, Astrophysics and Space Science Library **326**, 1 (2007).
[17] J. L. Friedman and N. Stergioulas, *Rotating Relativistic Stars* (Cambridge University Press, Cambridge, England, 2013).
[18] G. Baym, T. Hatsuda, T. Kojo, P. D. Powell, Y. Song, and T. Takatsuka, Rep. Prog. Phys. **81**, 056902 (2018).
[19] J. M. Lattimer and M. Prakash, Science **304**, 536 (2004).
[20] G. J. Olmo, D. Rubiera-Garcia, and A. Wojnar, Phys. Rep. **876**, 1 (2020).
[21] J. M. Lattimer, Annu. Rev. Nucl. Part. Sci. **62**, 485 (2012).
[22] A. W. Steiner and S. Gandolfi, Phys. Rev. Lett. **108**, 081102 (2012).
[23] C. J. Horowitz, M. A. Perez-Garcia, D. K. Berry, and J. Piekarewicz, Phys. Rev. C **72**, 035801 (2005).
[24] G. Watanabe, K. Iida, and K. Sato, Nucl. Phys. **A676**, 455 (2000); **A726**, 357(E) (2003).
[25] H. Shen, H. Toki, K. Oyamatsu, and K. Sumiyoshi, Nucl. Phys. **A637**, 435 (1998).
[26] J. Xu, L. W. Chen, B. A. Li, and H. R. Ma, Astrophys. J. **697**, 1549 (2009).
[27] K. Hebeler, J. M. Lattimer, C. J. Pethick, and A. Schwenk, Astrophys. J. **773**, 11 (2013).
[28] J. de Jesús Mendoza-Temis, M. R. Wu, G. Martínez-Pinedo, K. Langanke, A. Bauswein, and H. T. Janka, Phys. Rev. C **92**, 055805 (2015).
[29] W. C. G. Ho, K. G. Elshamouty, C. O. Heinke, and A. Y. Potekhin, Phys. Rev. C **91**, 015806 (2015).
[30] A. Kanakis-Pegios, P. S. Koliogiannis, and C. C. Moustakidis, Symmetry **13**, 183 (2021).
[31] L. Tsaloukidis, P. S. Koliogiannis, A. Kanakis-Pegios, and C. C. Moustakidis, Phys. Rev. D **107**, 023012 (2023).
[32] M. Buschmann, R. T. Co, C. Dessert, and B. R. Safdi, Phys. Rev. Lett. **126**, 021102 (2021).
[33] B. R. Safdi, Z. Sun, and A. Y. Chen, Phys. Rev. D **99**, 123021 (2019).
[34] A. Hook, Y. Kahn, B. R. Safdi, and Z. Sun, Phys. Rev. Lett. **121**, 241102 (2018).
[35] T. D. P. Edwards, B. J. Kavanagh, L. Visinelli, and C. Weniger, Phys. Rev. Lett. **127**, 131103 (2021).
[36] S. Nurmi, E. D. Schiappacasse, and T. T. Yanagida, J. Cosmol. Astropart. Phys. 09 (2021) 004.
[37] A. V. Astashenok, S. Capozziello, S. D. Odintsov, and V. K. Oikonomou, Phys. Lett. B **811**, 135910 (2020).
[38] A. V. Astashenok, S. Capozziello, S. D. Odintsov, and V. K. Oikonomou, Phys. Lett. B **816**, 136222 (2021).
[39] S. Capozziello, M. De Laurentis, R. Farinelli, and S. D. Odintsov, Phys. Rev. D **93**, 023501 (2016).
[40] A. V. Astashenok, S. Capozziello, and S. D. Odintsov, J. Cosmol. Astropart. Phys. 01 (2015) 001.
[41] A. V. Astashenok, S. Capozziello, and S. D. Odintsov, Phys. Rev. D **89**, 103509 (2014).
[42] A. V. Astashenok, S. Capozziello, and S. D. Odintsov, J. Cosmol. Astropart. Phys. 12 (2013) 040.
[43] A. S. Arapoglu, C. Deliduman, and K. Y. Eksi, J. Cosmol. Astropart. Phys. 07 (2011) 020.
[44] G. Panotopoulos, T. Tangphati, A. Banerjee, and M. K. Jasim, Phys. Lett. B **817**, 136330 (2021).
[45] R. Lobato, O. Lourenço, P. H. R. S. Moraes, C. H. Lenzi, M. de Avellar, W. de Paula, M. Dutra, and M. Malheiro, J. Cosmol. Astropart. Phys. 12 (2020) 039.
[46] K. Numajiri, T. Katsuragawa, and S. Nojiri, Phys. Lett. B **826**, 136929 (2022).

[47] S. Altiparmak, C. Ecker, and L. Rezzolla, Astrophys. J. Lett. **939**, L34 (2022).
[48] A. Bauswein, G. Guo, J. H. Lien, Y. H. Lin, and M. R. Wu, Phys. Rev. D **107**, 083002 (2023).
[49] S. Vretinaris, N. Stergioulas, and A. Bauswein, Phys. Rev. D **101**, 084039 (2020).
[50] A. Bauswein, S. Blacker, V. Vijayan, N. Stergioulas, K. Chatziioannou, J. A. Clark, N. U. F. Bastian, D. B. Blaschke, M. Cierniak, and T. Fischer, Phys. Rev. Lett. **125**, 141103 (2020).
[51] A. Bauswein, O. Just, H. T. Janka, and N. Stergioulas, Astrophys. J. Lett. **850**, L34 (2017).
[52] E. R. Most, L. R. Weih, L. Rezzolla, and J. Schaffner-Bielich, Phys. Rev. Lett. **120**, 261103 (2018).
[53] L. Rezzolla, E. R. Most, and L. R. Weih, Astrophys. J. Lett. **852**, L25 (2018).
[54] A. Nathanail, E. R. Most, and L. Rezzolla, Astrophys. J. Lett. **908**, L28 (2021).
[55] S. Köppel, L. Bovard, and L. Rezzolla, Astrophys. J. Lett. **872**, L16 (2019).
[56] G. Raaijmakers, S. K. Greif, K. Hebeler, T. Hinderer, S. Nissanke, A. Schwenk, T. E. Riley, A. L. Watts, J. M. Lattimer, and W. C. G. Ho, Astrophys. J. Lett. **918**, L29 (2021).
[57] E. R. Most, L. J. Papenfort, S. Tootle, and L. Rezzolla, Astrophys. J. **912**, 80 (2021).
[58] C. Ecker and L. Rezzolla, Mon. Not. R. Astron. Soc. **519**, 2615 (2022).
[59] J. L. Jiang, C. Ecker, and L. Rezzolla, arXiv:2211.00018.
[60] P. Pani and E. Berti, Phys. Rev. D **90**, 024025 (2014).
[61] K. V. Staykov, D. D. Doneva, S. S. Yazadjiev, and K. D. Kokkotas, J. Cosmol. Astropart. Phys. 10 (2014) 006.
[62] M. Horbatsch, H. O. Silva, D. Gerosa, P. Pani, E. Berti, L. Gualtieri, and U. Sperhake, Classical Quantum Gravity **32**, 204001 (2015).
[63] H. O. Silva, C. F. B. Macedo, E. Berti, and L. C. B. Crispino, Classical Quantum Gravity **32**, 145008 (2015).
[64] D. D. Doneva, S. S. Yazadjiev, N. Stergioulas, and K. D. Kokkotas, Phys. Rev. D **88**, 084060 (2013).
[65] R. Xu, Y. Gao, and L. Shao, Phys. Rev. D **102**, 064057 (2020).
[66] M. Salgado, D. Sudarsky, and U. Nucamendi, Phys. Rev. D **58**, 124003 (1998).
[67] M. Shibata, K. Taniguchi, H. Okawa, and A. Buonanno, Phys. Rev. D **89**, 084005 (2014).
[68] A. Savaş Arapoğlu, K. Yavuz Ekşi, and A. Emrah Yükselci, Phys. Rev. D **99**, 064055 (2019).
[69] F. M. Ramazanoğlu and F. Pretorius, Phys. Rev. D **93**, 064005 (2016).
[70] Z. Altaha Motahar, J. L. Blázquez-Salcedo, D. D. Doneva, J. Kunz, and S. S. Yazadjiev, Phys. Rev. D **99**, 104006 (2019).
[71] X. Y. Chew, V. Dzhunushaliev, V. Folomeev, B. Kleihaus, and J. Kunz, Phys. Rev. D **100**, 044019 (2019).
[72] J. L. Blázquez-Salcedo, F. Scen Khoo, and J. Kunz, Europhys. Lett. **130**, 50002 (2020).
[73] Z. Altaha Motahar, J. L. Blázquez-Salcedo, B. Kleihaus, and J. Kunz, Phys. Rev. D **96**, 064046 (2017).
[74] S. D. Odintsov and V. K. Oikonomou, Phys. Dark Universe **32**, 100805 (2021).
[75] S. D. Odintsov and V. K. Oikonomou, Ann. Phys. (Amsterdam) **440**, 168839 (2022).
[76] V. K. Oikonomou, Classical Quantum Gravity **38**, 175005 (2021).
[77] J. M. Z. Pretel, J. D. V. Arbañil, S. B. Duarte, S. E. Jorás, and R. R. R. Reis, J. Cosmol. Astropart. Phys. 09 (2022) 058.
[78] J. M. Z. Pretel and S. B. Duarte, Classical Quantum Gravity **39**, 155003 (2022).
[79] R. R. Cuzinatto, C. A. M. de Melo, L. G. Medeiros, and P. J. Pompeia, Phys. Rev. D **93**, 124034 (2016); **98**, 029901 (E) (2018).
[80] V. K. Oikonomou, Mon. Not. R. Astron. Soc. **520**, 2934 (2023).
[81] Y. Akrami *et al.* (Planck Collaboration), Astron. Astrophys. **641**, A10 (2020).
[82] R. Kallosh, A. Linde, and D. Roest, J. High Energy Phys. 09 (2014) 062.
[83] R. Kallosh and A. Linde, J. Cosmol. Astropart. Phys. 07 (2013) 002.
[84] S. Ferrara, R. Kallosh, A. Linde, and M. Porrati, Phys. Rev. D **88**, 085038 (2013).
[85] R. Kallosh, A. Linde, and D. Roest, J. High Energy Phys. 11 (2013) 198.
[86] A. Linde, J. Cosmol. Astropart. Phys. 05 (2015) 003.
[87] S. Cecotti and R. Kallosh, J. High Energy Phys. 05 (2014) 114.
[88] J. J. M. Carrasco, R. Kallosh, and A. Linde, J. High Energy Phys. 10 (2015) 147.
[89] J. J. M. Carrasco, R. Kallosh, A. Linde, and D. Roest, Phys. Rev. D **92**, 041301 (2015).
[90] R. Kallosh, A. Linde, and D. Roest, Phys. Rev. Lett. **112**, 011303 (2014).
[91] D. Roest and M. Scalisi, Phys. Rev. D **92**, 043525 (2015).
[92] R. Kallosh, A. Linde, and D. Roest, J. High Energy Phys. 08 (2014) 052.
[93] J. Ellis, D. V. Nanopoulos, and K. A. Olive, J. Cosmol. Astropart. Phys. 10 (2013) 009.
[94] Y. F. Cai, J. O. Gong, and S. Pi, Phys. Lett. B **738**, 20 (2014).
[95] Z. Yi and Y. Gong, Phys. Rev. D **94**, 103527 (2016).
[96] Y. Akrami, R. Kallosh, A. Linde, and V. Vardanyan, J. Cosmol. Astropart. Phys. 06 (2018) 041.
[97] S. Qummer, A. Jawad, and M. Younas, Int. J. Mod. Phys. D **29**, 2050117 (2020).
[98] Q. Fei, Z. Yi, and Y. Yang, Universe **6**, 213 (2020).
[99] A. D. Kanfon, F. Mavoa, and S. M. J. Houndjo, Astrophys. Space Sci. **365**, 97 (2020).
[100] I. Antoniadis, A. Karam, A. Lykkas, T. Pappas, and K. Tamvakis, Proc. Sci. CORFU2019 (**2020**) 073.
[101] C. García-García, P. Ruíz-Lapuente, D. Alonso, and M. Zumalacárregui, J. Cosmol. Astropart. Phys. 07 (2019) 025.
[102] F. X. Linares Cedeño, A. Montiel, J. C. Hidalgo, and G. Germán, J. Cosmol. Astropart. Phys. 08 (2019) 002.
[103] S. Karamitsos, J. Cosmol. Astropart. Phys. 09 (2019) 022.
[104] D. D. Canko, I. D. Gialamas, and G. P. Kodaxis, Eur. Phys. J. C **80**, 458 (2020).
[105] T. Miranda, C. Escamilla-Rivera, O. F. Piattella, and J. C. Fabris, J. Cosmol. Astropart. Phys. 05 (2019) 028.

[106] A. Karam, T. Pappas, and K. Tamvakis, J. Cosmol. Astropart. Phys. 02 (2019) 006.
[107] K. Nozari and N. Rashidi, Astrophys. J. **863**, 133 (2018).
[108] C. García-García, E. V. Linder, P. Ruíz-Lapuente, and M. Zumalacárregui, J. Cosmol. Astropart. Phys. 08 (2018) 022.
[109] N. Rashidi and K. Nozari, Int. J. Mod. Phys. D **27**, 1850076 (2018).
[110] Q. Gao, Y. Gong, and Q. Fei, J. Cosmol. Astropart. Phys. 05 (2018) 005.
[111] K. Dimopoulos, L. Donaldson Wood, and C. Owen, Phys. Rev. D **97**, 063525 (2018).
[112] T. Miranda, J. C. Fabris, and O. F. Piattella, J. Cosmol. Astropart. Phys. 09 (2017) 041.
[113] A. Karam, T. Pappas, and K. Tamvakis, Phys. Rev. D **96**, 064036 (2017).
[114] K. Nozari and N. Rashidi, Phys. Rev. D **95**, 123518 (2017).
[115] Q. Gao and Y. Gong, Eur. Phys. J. Plus **133**, 491 (2018).
[116] C. Q. Geng, C. C. Lee, and Y. P. Wu, Eur. Phys. J. C **77**, 162 (2017).
[117] S. D. Odintsov and V. K. Oikonomou, Phys. Lett. B **807**, 135576 (2020).
[118] S. D. Odintsov and V. K. Oikonomou, Phys. Rev. D **94**, 124026 (2016).
[119] S. D. Odintsov and V. K. Oikonomou, Classical Quantum Gravity **34**, 105009 (2017).
[120] L. Järv, A. Karam, A. Kozak, A. Lykkas, A. Racioppi, and M. Saal, Phys. Rev. D **102**, 044029 (2020).
[121] J. S. Read, B. D. Lackey, B. J. Owen, and J. L. Friedman, Phys. Rev. D **79**, 124032 (2009).
[122] J. S. Read, C. Markakis, M. Shibata, K. Uryu, J. D. E. Creighton, and J. L. Friedman, Phys. Rev. D **79**, 124033 (2009).
[123] F. Douchin and P. Haensel, Astron. Astrophys. **380**, 151 (2001).
[124] A. Akmal, V. R. Pandharipande, and D. G. Ravenhall, Phys. Rev. C **58**, 1804 (1998).
[125] R. B. Wiringa, V. Fiks, and A. Fabrocini, Phys. Rev. C **38**, 1010 (1988).
[126] L. Engvik, G. Bao, M. Hjorth-Jensen, E. Osnes, and E. Ostgaard, Astrophys. J. **469**, 794 (1996).
[127] H. Müther, M. Prakash, and T. L. Ainsworth, Phys. Lett. B **199**, 469 (1987).
[128] H. Mueller and B. D. Serot, Nucl. Phys. **A606**, 508 (1996).
[129] A. Akmal and V. R. Pandharipande, Phys. Rev. C **56**, 2261 (1997).
[130] R. Arnowitt, S. Deser, and C. W. Misner, Phys. Rev. **118**, 1100 (1960).
[131] M. C. Miller, F. K. Lamb, A. J. Dittmann, S. Bogdanov, Z. Arzoumanian, K. C. Gendreau, S. Guillot, W. C. G. Ho, J. M. Lattimer, M. Loewenstein *et al.*, Astrophys. J. Lett. **918**, L28 (2021).
[132] D. I. Kaiser, Phys. Rev. D **52**, 4295 (1995).
[133] Valerio Faraoni, *Cosmology in Scalar-Tensor Gravity* (Springer, New York, 2004).
[134] V. Faraoni, Galaxies **1**, 96 (2013).
[135] M. Buck, M. Fairbairn, and M. Sakellariadou, Phys. Rev. D **82**, 043509 (2010).
[136] V. Faraoni, Phys. Rev. D **53**, 6813 (1996).
[137] S. Sonego and V. Faraoni, Classical Quantum Gravity **10**, 1185 (1993).
[138] M. F. O'Boyle, C. Markakis, N. Stergioulas, and J. S. Read, Phys. Rev. D **102**, 083027 (2020).
[139] L. Lindblom, Phys. Rev. D **82**, 103011 (2010).
[140] V. K. Oikonomou, Classical Quantum Gravity **40**, 085005 (2023).
[141] S. D. Odintsov and V. K. Oikonomou, Int. J. Mod. Phys. D **32**, 2250135 (2023).
[142] S. S. Mishra, V. Sahni, and A. V. Toporensky, Phys. Rev. D **98**, 083538 (2018).
[143] Nikolaos Stergioulas, https://github.com/niksterg.
[144] C. E. Rhoades, Jr. and R. Ruffini, Phys. Rev. Lett. **32**, 324 (1974).
[145] V. Kalogera and G. Baym, Astrophys. J. Lett. **470**, L61 (1996).
[146] T. Soultanis, A. Bauswein, and N. Stergioulas, Phys. Rev. D **105**, 043020 (2022).